Article:
Ahmed, A, Nawaz, R, Drake, F orcid.org/0000-0003-1442-5950 et al. (1 more author) (2018) Modelling land susceptibility to erosion in the coastal area of Bangladesh: A geospatial approach. Geomorphology, 320. pp. 82-97. ISSN 0169-555X

https://doi.org/10.1016/j.geomorph.2018.08.004

Modelling land susceptibility to erosion in the coastal area of Bangladesh: A geospatial approach

ABSTRACT

This research aimed to develop a widely applicable raster GIS-based model for analysing susceptibility of coastal lands to erosion. The model, Land Susceptibility to Coastal Erosion (LSCE), was applied for the coastal area of Bangladesh as a case study. This study included three coastal zones (western, central and eastern) that cover the entire coastal area of the country. The outputs of the model comprised physical susceptibility of the coastal lands to erosion according to five susceptibility classes. The overall results demonstrate that out of the entire coastal area about 0.59 % (266.32 km²) and 0.02 % (10.01 km²) of the coastal lands exhibit high and very high susceptibility to erosion, respectively. These make 276.33 km² in total as being highly susceptible to erosion, which is noteworthy for the densely populated coastal area of the country. The remaining 5.49 %, 20.56 % and 73.34 % of lands were identified as having moderate, low and very low susceptibility to erosion, respectively. The developed model is highly suitable for addressing the impacts of hydro-climatic parameters on susceptibility to coastal erosion. Hence, this study identified and mapped the influence of hydro-climatic parameters on the coast by assessing seasonal variations of susceptibility to erosion. The outputs were then validated by developing an inventory map and analysing the independent historical observations by using 'degree of fit' curves. The LSCE model could be useful for coastal researchers in assessing erosion susceptibility of dynamic coastal lands around the world.

Key words: coast; erosion; LSCE; susceptibility.

1. Introduction

Coastal areas form a dynamic part of the world and exhibit behaviour as a multi-functional complex system (Ramieri et al., 2011). Due to climate change, sea-level rise and extreme weather events, coastal systems are continuously being affected by natural hazards and respond in different ways (Balica et al., 2012). Coastal erosion is being treated as a serious morpho-dynamic hazard in coastal areas around the world (Addo et al., 2008). The coastal area of Bangladesh is particularly dynamic where land erosion and accretion are taking place at different rates (Brammer, 2014). The coastal area of the country is densely populated (949 persons/km^2) (Islam, 2004). However, the assessment of physical susceptibility to erosion is of significant importance in managing coastal land and formulating policies and mitigation plans (Cai et al., 2016).

Global (Gornitz, 1990; Klein and Nicholls, 1999) as well as regional (Bryan et al., 2001; Dawson et al., 2009) approaches have been used widely for assessing the degree of coastal erosion (McLaughlin and Cooper, 2010). These approaches can be grouped into three main categories (Ramieri et al., 2011): Geographic Information System (GIS) based Decision Support Systems (e.g. DESYCO, DITTY-DSS), Dynamic Computer Modelling (e.g. DIVA, RACE, Delft3D, RegIS, SimCLIM), and index- or indicator-based methods (e.g. CVI, Composite Vulnerability Index, Multi-scale Coastal Vulnerability Index). Moreover, the use of satellite images have been used that are convenient in identifying the pattern of land dynamics (area and rate of eroded and accreted lands) and useful for extracting information that can be of value in assessing coastal erosion. However, the approaches do not provide readily available information for erosion susceptibility and are not suitable for assessing the level of physical susceptibility of coastal lands to erosion (Ahmed et al., 2018). Hence, it is imperative to develop models that are capable of incorporating both spatial and temporal aspects of land susceptibility to erosion (van Westen, 2000; Boori, 2010). The use of GIS in developing susceptibility models has received much attention in recent times (Van Westen, 2000; Chung and Fabbri, 2003) and hence can be regarded as an important tool for such analysis (Chung

and Fabbri, 2003). GIS can be an efficient way of analysing coastal land susceptibility by way of selecting parameters, assigning parameter weights, interpolating pixels and presenting maps under a model domain (Boori, 2010).

Assessment of erosion susceptibility at large spatial scales (global) is quite ineffective since coastal processes are complex, being highly influenced by local factors and requires a large amount of data in GIS-based models (Fitton et al., 2016). There are a number of GIS-based studies conducted on coastal erosion at regional and local scales (Dolan et al.,1980; Saha and Singh, 1991; White and El-Asmar, 1999; Shifeng et al., 2002; Azab and Noor, 2003; Potdar et al., 2003; Wang, 2003; Zoran and Anderson, 2006; Hegde and Reju, 2007; Jimmy, 2010; Prabaharan et al., 2010; Alves et al., 2011; Iqubal and Ali, 2011; Lins-de-Barros and Muehe, 2011; Shibly and Takewaka, 2012; Alam and Uddin, 2013; Chowdhury and Tripathi, 2013; Islam et al., 2013; Sarwar and Woodroffe, 2013; Fernandez-Nunez et al., 2015; Reeder-Myers, 2015). Most of the studies, however, identified coastal erosion by lines in vector-based GIS model (Harvey and Woodroffe, 2008; Lins-de-Barros and Muehe, 2011). The problem of dealing with vector-based outputs of coastal erosion is that the vector lines only represent the shorelines and exclude information on offshore and inland conditions (Fitton et al., 2016). Inland conditions are essential in assessing coastal susceptibility to erosion (Fitton et al., 2016). However, the assessment of both offshore and inland conditions of coastal land susceptibility to erosion is convenient to interpret by using a pixel (or cell) based GIS model.

The evaluation of physical elements (e.g. surface elevation, bathymetry, soil characteristics, geomorphic features etc.) is important in assessing erosion susceptibility (MPI, 2017). Additionally, hydro-climatic factors (e.g. water discharge, mean sea level, rainfall etc.) have substantial impacts on physical susceptibility to erosion and their influences are likely to increase in future (Warrick and Ahmad, 1996; Fitzgerald et al., 2008). However, existing physical conditions of any coastal system exert significant control over the impacts of hydro-

climatic factors. For instance, geomorphic characteristics have a substantial influence on rapid runoff generation and movement of water through the drainage network in a coastal area (Naylor et al., 2017). Moreover, human interventions such as construction of defence structures (e.g. revetment, polder), land reclamation and afforestation (e.g. mangrove plantation) have significant impacts on overall susceptibility of coastal lands to erosion (Hegde, 2010). As far as the authors are aware, a raster GIS-based study on assessing inland and offshore (i.e. islands) conditions of erosion susceptibility by addressing both physical elements and hydro-climatic conditions has not been done before. The study conducted by McLaughlin and Cooper (2010) emphasised tidal and wave heights as coastal forcing in classifying vulnerability of coastal lands by using an index-based approach. The studies of Alves et al. (2011) and Fitton et al. (2016) dealt with a pixel-based GIS model in assessing coastal erosion at local and regional scales, but these studies did not incorporate the impacts of hydro-climatic triggering factors in the assessments. However, considering the shortcomings of the above-mentioned literature, this study formulated the research question as: how best to address the compelling factors in assessing land susceptibility to coastal erosion?

This research described herein developed a widely applicable raster GIS-based model, namely Land Susceptibility to Coastal Erosion (LSCE), to analyse coastal physical susceptibility to erosion. The current research is an improvement on previous methods in assessing land susceptibility to coastal erosion because of its inclusion of both physical elements and hydro-climatic factors in the assessment. Moreover, the developed model is highly suitable for addressing the impacts of hydro-climatic parameters on physical susceptibility to erosion, and broadens the opportunity for predicting future land susceptibility to coastal erosion around the world by incorporating future scenarios of hydro-climatic factors in the model. The LSCE model is applied here for the coastal area of Bangladesh as a case study. Previous GIS-based studies (Saha and Singh, 1991; Potdar et al., 2003; Prabaharan et al., 2010; Iqubal and Ali, 2011; Shibly and Takewaka, 2012; Alam and Uddin, 2013; Islam

et al., 2013; Sarwar and Woodroffe, 2013) have assessed shoreline retreat and the rate of erosion and accretion in the coastal area of Bangladesh and the Bay of Bengal region. However, the present research analysed the spatial (i.e. inland and offshore islands) and temporal (i.e. seasonal variations) aspects of existing land susceptibility to erosion in the study area. The research is also unique for the area in that it includes the seasonal impacts of hydro-climatic factors on physical susceptibility to erosion.

2. Methodology

2.1. Study area

To apply the LSCE model this research considered the entire coastal lands of Bangladesh as a study area (Fig. 1). The reason for choosing the study area lies on the fact of its dynamic nature and increased impacts of hydro-climatic factors. The total area is 47,200 km² (MoEF, 2007) that includes the lands (including islands), internal rivers, estuarine and nearshore water bodies. Furthermore, the area encompasses diverse characteristics of natural coastal systems (IPCC, 2007 a, b) such as beaches, delta, estuary, lagoons and mangroves etc. It accounts for 32 % of the total area of the country (Islam, 2004). This study identified a total 45,220 km² of land area for assessment and excluded all types of water bodies from the analysis. The coastal area of the country can be divided into three zones: the western, central and eastern on the basis of geomorphological characteristics (Shibly and Takewaka, 2012) that cover approximately 27,150 km², 12,040 km² and 8,010 km² of coastal land area, respectively. Based on the exposure to the Bay of Bengal, the coastal area has also been subdivided into interior coast (23,265 km²) and exterior coast (23,935 km²) (PDO-ICZMP, 2006; Islam et al., 2006). The interior coast experiences direct influences of water discharge from coastal rivers, wave action and indirect influences of tidal movement and sea-level rise. However, the exterior coast is directly influenced by the Bay of Bengal and lower estuary of the Meghna river (MoWR, 2005) and experiences the maximum limit of tidal movement, sea-level rise, wave action etc. (PDO-ICZMP, 2006). Since the coastal area is a physical entity, the inland

boundary of the area was fixed based on both of these direct and indirect influences (PDO-ICZMP, 2006).

The physical and hydro-climatic settings of the coastal area are highly diverse. Most of the areas in the western and central coastal zones are low-lying, being at altitudes between 0 and 6 m, but the heights in the eastern coastal zone range from 0 to 327 m above mean sea level (USGS, 2017). The nearshore bathymetric depths vary from 0 to -45 m for the three coastal zones (MGDS, 2017). The Meghna estuary area represents higher bathymetric depths comparing to other areas in the central coastal zone. Furthermore, the types of surface geology and geomorphic features are not uniform for the entire coastal area. The interior part is mostly formed by Pleistocene and Pliocene formations, deltaic silt and marsh clay and peat. The areas close to the Bay of Bengal are formed by estuarine deposits, Pleistocene and Neogene formations, tidal deltaic deposits and tidal muds. Most of the coastal soils (i.e. about 63%) are moderate to highly permeable. However, the hydro-climatic features of the area substantially vary between the zones and the seasons. The average discharge of 29.07 m^3/s from the coastal rivers during winter season reached as high as 65396.12 m^3/s during the monsoon season in 2015 (BWDB, 2016). In addition, seasonal variation in mean sea level in the coastal area is significant that ranges from 1.61 m during winter to 2.76 m during monsoon season (BIWTA, 2017; PSMSL, 2017; UHSLC, 2017). The average rainfall in the area was recorded as 123 to 301 mm in 2015 but this amount of rainfall fluctuates between seasons (BMD, 2016). Seasonally, the lowest rainfall recorded during winter ranges from 10.22 to 16.79 mm, whereas highest rainfall occurred during the monsoon ranges from 300 to 896 mm on average. The average wind speed in the area varied from 0.36 m/s during the post-monsoon to 3.84 m/s during the monsoon in 2015 (BMD, 2016). The south-asian monsoon winds dominate in the area in which approximately 37% and 31% (68% in total) winds blow from southwest and south directions respectively (BMD, 2016). Remaining 32% annual average winds blow from north, northwest and southeast directions. For instance, 45%, 54% and 53%

of annual average winds blown over the Khulna, Barisal and Chittagong coastal areas, respectively, from south, southwest and southeast directions (BMD, 2016; Global Wind Atlas, 2017). During pre-monsoon and monsoon seasons, strong winds blow from southwest and south directions respectively whereas, weak winds blow from north direction during winter season (IWFM, 2012). Wind speeds during post-monsoon period are moderate and blow from lands (i.e. from northwest direction). Tides in this area are semi-diurnal (Islam et al., 2016). Tidal currents can be as fast as 3 m/s, as observed in Sandwip and Hatiya channels (Barua, 1997). However, the longshore currents travel anti-clockwise in the area and are influenced by tidal bores and waves (Krantz, 1999).

The selection of the study area is also significant from a risk management perspective. The population in the area comprises about 28 % of total population of the country (Islam, 2004). The population has increased in the area from only 8.1 million a century earlier (WARPO, 2004) to about 50 million during recent times (BBS, 2015). Due to fertile lands and abundance of livelihood options, this number is expected to be around 57.9 million by 2050 (Minar et al., 2013). The density of population varies between the coast zones. The density varies from 688 to 1935 people/km^2 in the eastern and central coastal districts such as Chittagong, Feni, Chandpur, Cox's Bazar, Laxmipur and Noakhali, whereas the western zone contains about 87 - 687 people/km^2 (BBS, 2011).

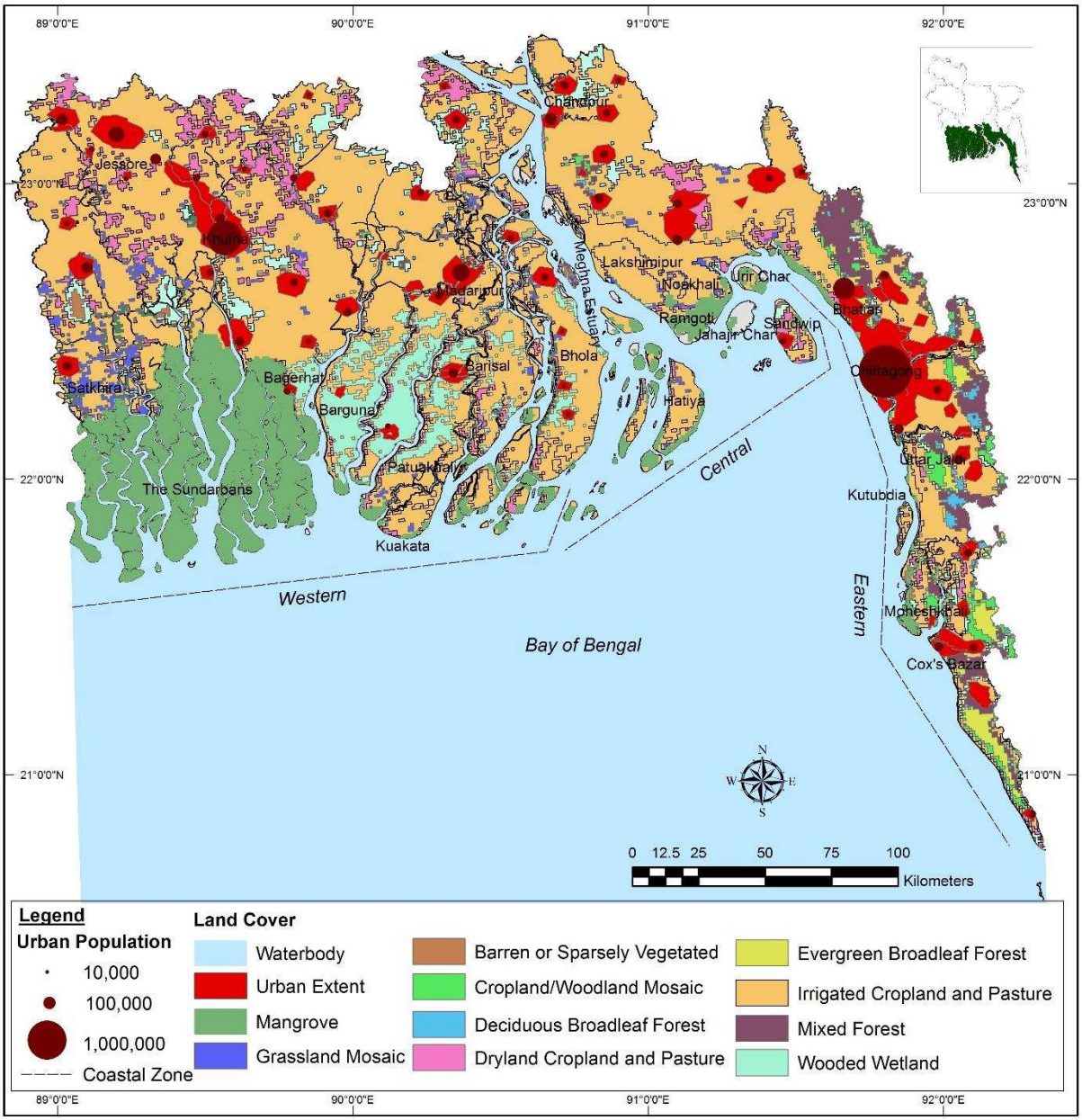

Fig.1. The study area (coastal area of Bangladesh). The figure shows the presence of major land cover categories in the area. A large part of the western coastal zone is covered by mangrove vegetation. However, the urban areas and their population are noteworthy in the coastal area.

2.2. Model parameters

Since land susceptibility to coastal erosion is largely determined by predispositions, preparatory and triggering factors (Saunders and Glassey, 2007; MPI, 2017), this study

identified nine parameters among which five are the underlying physical elements (which can be considered as predispositions): surface elevation, surface geology, bathymetry, soil permeability and distance from shoreline. The remaining four parameters are the hydro-climatic triggering factors: discharge of coastal river water, mean sea level, rainfall and wind speed and direction (Fig. 2). Moreover, this study addressed the role of preparatory factors on land susceptibility to coastal erosion. The preparatory factors are the actions and interventions that may place a land unit at higher or lower likelihood of erosion (MPI, 2017). The study addressed two types of preparatory factors: natural (i.e. sedimentation) and human-induced (i.e. defence structures).

The model parameters were identified and selected through an in-depth review of relevant literature (Viles and Spencer, 1995; Barua, 1997; Krantz, 1999; Ali, 1999; Mikhailov and Dotsenko 2007; Parvin et al., 2008; Masatomo, 2009; Rabbani et al., 2010; Hossain, 2012; Chowdhury, 2013; Brammer, 2014) available for the study area. However, relevant literature (Umitsu, 1997; Ahmed, 1999; Ali, 1999; Huq et al., 1999; Krantz, 1999; RRCAP, 2001; Islam, 2006; Karim and Mimura, 2006; Palinkas et al., 2006; Ali et al., 2007; Mikhailov and Dotsenko 2007; Shamsuddoha and Chowdhury, 2007; Sokolewiczand-Louters, 2007; Unnikrishnan and Shankar, 2007; Bird, 2008; Islam, 2008; Parvin et al., 2008; Masatomo, 2009; Rabbani et al., 2010; SDC, 2010; Sarker et al., 2011; Hossain, 2012; Khan, 2012; Smith, 2012; Taguchi et al., 2013; Brammer, 2014; Islam et al., 2016) was consulted to justify the influence and interrelationships of the model parameters on land susceptibility to erosion in the coastal area. It is recognized that the higher surface elevations along with solid rock formations (Huq et al., 1999) and unbroken coast (Karim and Mimura, 2006) in the eastern coastal zone are less likely to erode compared to the western and central coastal zones. Previous studies (Sarker et al., 2011; Islam et al., 2016) suggest that the nearshore bathymetric depths have significant influences on the pattern and rate of erosion in the coastal area. The pattern of sediment distribution in the area are largely influenced by the bathymetry and the forces of tides and

waves (Palinkas et al., 2006; Bird, 2008). The study considered the types of surface geology in which, major types of geomorphic features (e.g. sand dunes, tidal flood plains, estuarine flood plains, coastal plains, beaches, lagoons, inter-tidal wetlands etc.) and their influences on erosion susceptibility are evaluated (Table 1). It is evident that the soft and unconsolidated silt and clay sediments quickly response to the forces of coastal river water discharge in the area (Masatomo, 2009). The offshore islands in the coastal area are mostly formed of this type of sediments (Umitsu, 1997). Moreover, the permeability of water into the coastal soils is high. About 63 % of the coastal soils are inclined to moderate and rapid permeability classes among which about 94 % of the entire Meghna estuary area fall under moderate to rapid permeability classes (BARC, 2016).

The influences of hydro-climatic factors on erosion potential in the coastal area are significant (Huq et al., 1999). For instance, discharge of water from the coastal rivers can be considered as an active driving force of erosion in the area (Ali et al., 2007; Islam, 2008; Taguchi et al., 2013). Besides, continuous wave action is one of the most important factors of erosion susceptibility especially, in the central coastal zone (Ahmed, 1999). The prevailing southern and southwestern monsoon winds generate waves that largely affect the offshore islands located in the central coastal zone. This study evaluated the speed and directions of winds as a proxy for wave actions in the coastal area. Moreover, the rise of mean sea level in the Bay of Bengal region is evident (Unnikrishnan and Shankar, 2007; Smith, 2012; Brammer, 2014) that inundates new coastal lands and thus affects the lands by wave actions. The Ganges floodplains and the islands in the Meghna estuary have the high potential to be affected by the rising sea level in the coastal area (Brammer, 2014). Together with water discharge, wave actions and mean sea level rise, excessive amount of rainfall triggers the rate of erosion in the coastal area (Krantz, 1999). Moreover, significant seasonal variations were observed for the hydro-climatic triggering factors (Karntz, 1999; Hossain, 2012; Chowdhury, 2013; BWDB, 2016) in the coastal area and hence, the daily average data were segmented into four seasons

and applied in the model domain. In assessing seasonal variations, the effects of underlying physical elements and the preparatory factors were considered as static.

It is reported that the high volume of sediment supply mitigates erosion susceptibility in the Meghna estuary area (Mikhailov and Dotsenko 2007). During the monsoon season when the sediment fluxes from the rivers are high, the process of accretion dominates in the Meghna estuary (Sokolewiczand-Louters, 2007). Like sedimentation, the impacts of defence structures such as polder, dyke, embankment and land reclamation projects in the coastal area are evident from a previous study (MES II, 2001). For instance, immediately after building a number of cross dams during 1950s and 1960s in the Meghna river near Laksmipur, Noakhali and Feni districts by Bangladesh Water Development Board (BWDB) under the Land Reclamation Project (LRC), a considerable portion of landmass (900 km^2) accreted in the lower reach of the Meghna estuary (Islam, 2006; Khan, 2008).

2.3. Methods

The study addressed the impacts of predispositions, preparatory and triggering factors on land susceptibility to erosion in the coastal area by using LSCE raster GIS model (Fig. 2). The model evaluated the individual contributions of the parameters by preparing, scaling, weighting and overlaying raster surfaces on the selected parameters. The preparation of raster surfaces involved some pre-processing tasks on the collected images used for surface elevation, bathymetry and shoreline detection. The tasks included geometric (i.e. geo-referencing), radiometric (i.e. conversion of DN to radiance and then to Top of Atmosphere-TOA reflectance for shoreline detection) and atmospheric corrections (i.e. Dark Object Subtraction-DOS). The pixel values of the processed raster surfaces were then classified into five different susceptibility categories by using a scale ranging from 1 to 5 (where 1 represents very low and 5 represents very high susceptibility) (Table 1). To prepare the scale, this study assumed that the higher the values of surface elevation, bathymetric depths and distance from

the shoreline, the lower the susceptibility and vice versa. On the other hand, the higher the values of river water discharge, mean sea level, rainfall and wind speed, the higher the susceptibility to erosion and vice versa. However, scale values for surface geology were assigned to five susceptibility classes based on their resistence capacity to erosion suppported by relevant literature (Hossain, 2012; Chowdhury, 2013; Brammer, 2014). Similarly, the types of soil permeability (BARC, 2016) were segmented into five susceptibility classes in which, slow permeability designates low erosion susceptibility and vice versa. Based on the source (i.e. land or water), the southwestern and southern winds were assumed to be highly effective for generating waves and the northern and northwestern winds have less influence on waves. However, southeastern wind has moderate effects in generating waves in the central coastal zone.

Table 1: Scales used for the LSCE model to categorise the cell values of raster surfaces into five susceptibility classes.

Parameter	**Time period**	**Susceptibility category**				
		Very low (1)	**Low (2)**	**Moderate (3)**	**High (4)**	**Very high (5)**
Surface elevation (m)	Average and all seasons	>12	9-12	6-9	3-6	0-3
Surface geology (type)	Average and all seasons	Dihing and DupiTiila formation, Girujan Clay, Bhuban formation, BokaBil formation, Tipam Sandstone	Valley alluvium and colluvium, Tidal mud, Marsh clay and peat, Mangrove swamp deposits, Lakes	Estuarine deposits, Alluvial silt and clay, Chandina alluvium	Alluvial silt, Deltaic silt, Tidal deltaic deposits	Newly formed ocean and riverine deposits, Tidal sand, Deltaic sand, Beach and sand dune, Alluvial sand
Bathymetry (m)	Average and all seasons	> -20	(-15)- (-20)	(-10)- (-15)	(-5) – (-10)	< -5
Soil permeability (class)	Average and all seasons	Very slow	Slow	Mixed	Moderate	Rapid

Distance from the coastline (m)	Average and all seasons	> 400	300-400	200-300	100-200	< 100
River water discharge (m^3/s)	Average	13- 6152	6152- 12290	12290- 18429	18429- 24567	24567- 30706
	Winter	4- 1766	1766- 3529	3529- 5291	5291- 7054	7054- 8816
	Pre-monsoon	4- 2806	2806- 5608	5608- 8410	8410- 11212	11212- 14013
	Monsoon	29- 13102	13102- 26175	26175- 39249	39249- 52322	52322- 65396
	Post-monsoon	16- 6868	6868- 13721	13721- 20574	20574- 27427	27427- 34280
Mean Sea Level (m)	Average	1.84- 2.17	2.17- 2.50	2.50- 2.83	2.83- 3.20	3.20- 3.50
	Winter	1.61- 1.93	1.93- 2.25	2.25- 2.57	2.57- 2.89	2.89- 3.20
	Pre-monsoon	1.72- 2.10	2.10- 2.40	2.40- 2.73	2.73- 3.10	3.10- 3.41
	Monsoon	2.12- 2.44	2.44- 2.77	2.77- 3.11	3.11- 3.44	3.44- 3.78
	Post-monsoon	1.95- 2.26	2.26- 2.58	2.58- 2.89	2.89- 3.21	3.21- 3.53
Rainfall (mm)	Average	123- 158	158- 194	194- 230	230- 265	265- 301
	Winter	10.22- 11.53	11.53- 12.85	12.85- 14.16	14.16- 15.48	15.48- 16.79
	Pre-monsoon	90- 109	109- 128	128- 147	147- 167	167- 186
	Monsoon	303-421	421- 540	540- 659	659- 777	777- 896
	Post-monsoon	86- 104	104- 122	122- 140	140- 158	158- 176
Wind speed (m/s) and direction	Average	0.76- 1.16	1.16- 1.57	1.57- 1.98	1.98- 2.39	2.39- 2.79
	Winter	0.52- 0.81 N	0.81- 1.12 N	1.12- 1.40 N	1.40- 1.69 N	1.69- 1.99 N
	Pre-monsoon	1.15- 1.62 SW	1.62- 2.09 SW	2.09- 2.56 SW/SE	2.56- 3.03 SW	3.03- 3.49 SW
	Monsoon	0.96- 1.54 S	1.54- 2.11 S	2.11- 2.69 S	2.69- 3.26 S	3.26- 3.84 S
	Post-monsoon	0.36- 0.66 NW	0.66- 0.96 NW	0.96- 1.26 NW	1.26- 1.56 NW	1.56- 1.86 NW

It was necessary to assign weights of individual parameters for the LSCE model in ArcMap. This study incorporated ratings of relevant experts in assigning weights of the model parameters. To accomplish this, the study organised a workshop inviting 11 experts having

in-depth local knowledge on land susceptibility to coastal erosion. The experts were asked to rate the parameters on a scale of 0 to 1 where 0 indicates least weight and 1 indicates most weight of the parameters. The experts agreed on assigning full weight (1 in a range of 0 to 1) for the underlying physical elements. However, the assigned weights for the drivers of change varied due to the nature of influences of the hydro-climatic factors. The final weights of the parameters yielded as 0.84 weight for discharge of river water, 0.79 for mean sea level, 0.71 for rainfall and 0.65 for wind speed by averaging the weights given by individual experts.

This study incorporated the impacts of preparatory factors in the model domain by generating two sets of buffer zones: one for defence structures and another for sedimentation. These buffer zones are enclosed areas and termed as 'moderators' in the LSCE model. Since the moderators (i.e. defence structures and sedimentation) reduce erosion susceptibility of coastal lands, the buffer zones were assigned negative values followed by expert opinions, on a range from 1 to 5 based on their nature of impacts. A negative value (-3) was assigned for the accreted buffer zones that are within 200 m landward from the coastline. Negative values (-2) and (-1) were assigned for the two buffers consecutively next to the first buffer zone. However, two sets of buffer zone were applied for the coastal defences. A negative value (-5) was assigned to the buffer zones for hard defence (i.e. embankment, sea-wall, dyke) whereas, a negative value (-3) was set for soft defences (i.e. polder, dam). The pixels of the raster surfaces that overlapped with the buffer zones were then identified and the values were re-calculated by using 'raster calculator' tool in ArcMap. The re-calculated pixels were finally mosaicked with the generated raster surfaces for final susceptibility scores.

Immediately after scaling and weighting of the raster surfaces and then mosaicking the moderators, the model was run by using 'Model Builder' extension of ArcMap (version 10.4). To run the model, the 'weighted Sum' operation of ArcMap was used that overlaid the raster surfaces where each were multiplied by their given weights; finally summing them together.

The weighted sum scores of the raster surfaces were converted to a non-dimensional scale ranging from 0 to 100 by using the following equation (Equation 1):

$$\frac{\text{Aggregated Score} - \text{lowest score}}{\text{Range (difference between highest and lowest score)}} \times 100$$

The yielded scores were then presented by five susceptibility classes ranging from 1 to 5 where, 0-20 = 1 (very low), 20-40 = 2 (low), 40-60 = 3 (moderate), 60-80 = 4 (high) and 80-100 = 5 (very high). The same procedure was applied for the four identified seasons: winter (December to February), pre-monsoon (March to May), monsoon (June to September) and post-monsoon (October to November) with a view to address the seasonal variations of hydro-climatic factors on land susceptibility to coastal erosion.

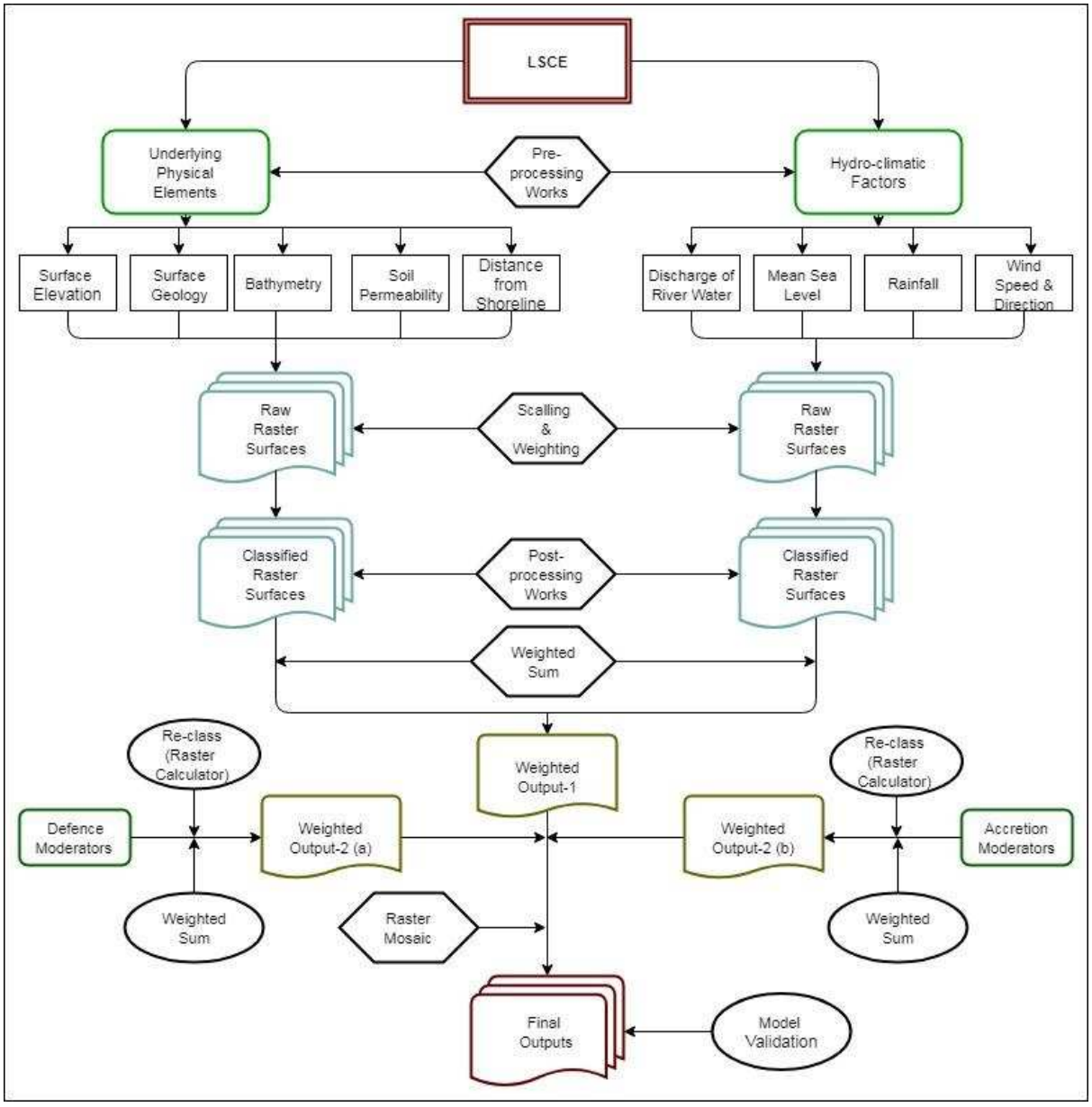

Fig. 2. A simplified representation of the processes involved in the LSCE model. The figure shows how the inclusion of climate-driven forces together with underlying physical elements in the model domain can obtain final outputs on erosion susceptibility.

2.4. Data sources

The spatial data for the underlying physical elements were collected from available secondary sources. Data on surface elevation were downloaded as ASTER-DEM (Advanced Space-born Thermal Emission and Reflection Radiometer-Digital Elevation Model) from United States

Geological Survey (USGS) Earth Explorer Global Visualization Viewer for the areal extent of study. The images having 30 m spatial resolution were used for further processing and analysis. Similarly, data on nearshore bathymetry for the entire coastal area were gathered from Global Multi-Resolution Topography (GMRT) synthesis by using 'GeoMapApp' (version 3.6.3) software tool. These data were cross-referenced with the data collected from Bangladesh Naval Force (BN, 2010; GMRT, 2017). Spatial dataset (i.e. shapefiles) on surface geology and associated geomorphic features was collected from United States Geological Survey (USGS, 2001), developed from Geological Survey of Bangladesh. Spatial dataset on soil permeability was collected from Bangladesh Agricultural Research Council (BARC, 2016). However, this study identified the existing shoreline with a view to measure the distances of each pixel from the shoreline. Hence, tide-synchronous Landsat (i.e. Landsat 8) satellite images were used to obtain the shoreline for the area. The use of satellite images to obtain shoreline is now well established (Boak and Turner, 2005). The benefit of using satellite images in identifying shoreline is that there is no need of fixing traditional benchmarks (known as proxies) such as high water line, datum based mean high water etc. (Boak and Turner, 2005). While using satellite images, the proxies depend on the definition of the shoreline and the image acquisition time. This study considered Mean High Water Level (MHWL) as the shoreline (line of demarcation between land and water). Only those images were selected that clearly represent MHWL in the images. Using OLI_TIRS sensor (Operational Land Imager_ Thermal Infrared Sensor), a total number of six images were collected to cover the entire coastal area (between path: 136-138 and row: 44-45). The acquisition date of the images was on 28 January 2015. Since Landsat satellite pass time over Bangladesh is between 10:00-10:30 (Islam, et al., 2016), all the images were selected based on the synchronization of satellite pass-time and high tide level. The images were collected on specific dates during the winter season (December to February) when most parts of the coastal lands were flood free. Hence, the shoreline during this season can clearly be discernible compared to the pre-monsoon, monsoon and post-monsoon seasons. The collected images were then mosaicked into a single image, georeferenced in the World Geodetic System (WGS84) datum and

projected using the Universal Transverse Mercator system (zone UTM 46 North). The McFeeters's Normalized Difference Water Index (NDWI) (McFeeters, 1996) was used to separate land from water body. The demarcated line between land and water was then digitised to identify the desired shoreline.

Data on mean sea level, rainfall and wind speed and direction were collected for the past thirty years from 1986 to 2015 (BMD, 2016; BIWTA, 2017; PSMSL, 2017; UHSLC, 2017;) whereas, data obtained for the discharge of coastal river water were available for past twenty years from 1996 to 2015 (BWDB, 2016). The average values of these data were used as existing conditions of the selected drivers. This study considered data for mean sea level collected from six stations located at Char Chenga, Chittagong, Cox's Bazar, Hiron Point, Khepupara and Sandwip in the coastal area of the country. These data were obtained from Bangladesh Inland Water Transport Authority (BIWTA), Permanent Solution for Mean Sea Level (PSMSL) and University of Hawaii Sea Level Centre (UHSLC). For rainfall and wind speed, this study analysed the data obtained from all 19 meteorological stations of the Bangladesh Meteorological Department (BMD) located in the coastal area of the country. A total of eleven stations of the Bangladesh Water Development Board (BWDB) were considered for the river discharge data that cover the major rivers, tributaries and distributaries in the coastal area.

2.5. Data processing and generation of raster surfaces

Considering the spatial extent of the area, the resolution of the raster surfaces was resampled to a 30x30 m (1 arc second) dimension (Fig. 3). It took 16 individual scenes of ASTER-DEM (60x60 km) to cover the surface elevations for the entire coastal area of the country. The initial vertical accuracy of the raw surface was ± 3.62 m. However, the mosaicked scene was first processed to remove artificial heights such as rooftops, construction works etc. (known as artifacts) from the original values by using the 'Majority Filter' in ArcMap. The Root Mean Square Error (RMSE) of the surface was then found to be ±0.28 m. The artifact-free raster

surface went through consistency checks with observed ground data. Hence, a total number of 90 sample spot heights were taken for the coastal area arbitarily from 1,711 vertical control points measured by Survey of Bangladesh (SoB, 2016). The correlation coefficient of Pearson's r between the sample heights and the corresponding heights of the ASTER-DEM was found to be 0.94 (p= 0.001 at 0.01 level of significance). The processed data showed surface elevations ranging from 0 to 327 m for the area studied. To evaluate the role of geomorphic features, the entire coastal land was segmented into 21 types of areas.

The shallow depths are the areas where the actions of waves are highly effective for potential erosion (Mazaheri and Ghaderi, 2011). In contrast, wave orbitals in deep water have less effects on erosion since, the orbitals do not touch the bed. Hence, this study considered shallow depths as high susceptibility to erosion and vice versa. The categorical values of nearshore bathymetric depths were transferred to the associated land areas to reflect the impact of bathymetric depths on that lands. The transformation process was accomplished by using 'Zonal Statistics' tool of ArcMap through creating 1000x1000 m fishnets for the whole coastal area attached to the waterbody. The use of zonal statistics is identical with the work of Islam et al. (2016) where statistics for target zones were calculated by a set of input zones (i.e. in this case, the land zones were considered as target and the bathymetric zones were as input zones). The reason for choosing 1000 m^2 fishnet was based on the conventional use (yet to be approved officially) of 500 m^2 set-back distance from shoreline for the study area. Since, wave actions at nearshore bathymetric zone are most likely to impact on associated lands (not essentially over the whole coastal area), the bathymetric values of input zones (i.e. 500 m^2 water body) were transferred to the target zones (i.e. 500 m^2 land area). However, to generate a raster surface on soil permeability, vector layers obtained from Bangladesh Agricultural Research Council (BARC) were converted into raster format using ArcMap. Likewise, raster surfaces for four hydro-climatic parameters were generated from point data by applying polynomial surface interpolation techniques in ArcMap. For instance, raster

surfaces for river discharges and mean sea level were generated by using krigging interpolation technique, whereas raster surfaces for rainfall and wind speed were generated by using Inverse Distance Weighting (IDW) interpolation technique in ArcMap. Like bathymetry, the values of river water discharges were transferred to the associated land area attached to the rivers by following the similar method used for bathymetry. However, generated raster surfaces for elevation and bathymetry went through some post-processing tasks by using 'rescale by function' and 'fill' operation in ArcMap to generalise the sinks and peaks by rounding nearest integer values.

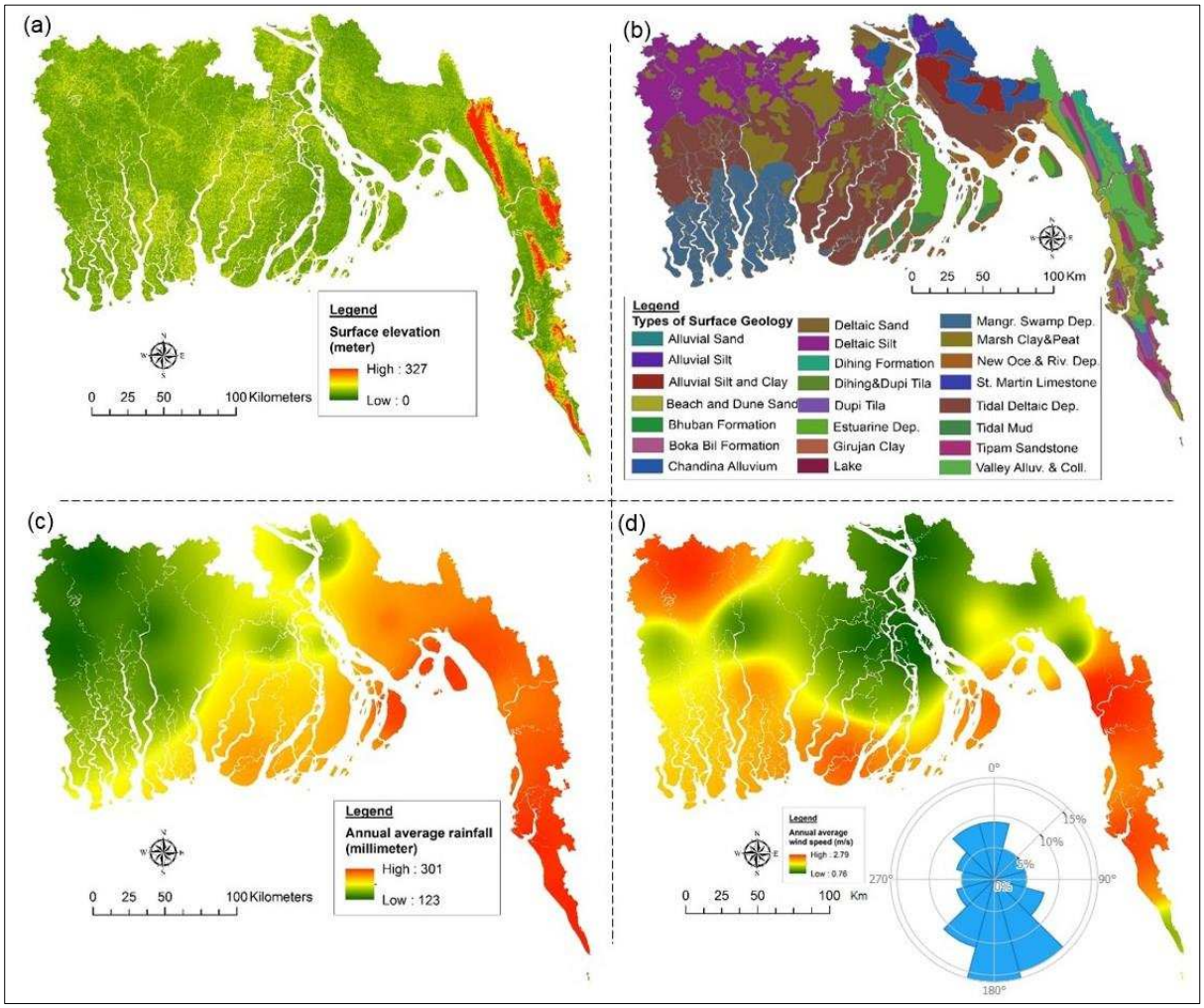

Fig. 3: Examples of some raster surfaces used for the LSCE model in which (a) represents the surface elevation, (b) major types of surface geology, (c) annual average rainfall, and (d) annual average wind speed and direction in the area.

2.6. Model validation

The validation of the outcomes of LSCE model was performed by using an inventory map of land erosion and accretion prepared from independent datasets. To prepare the inventory map, historical data collected from Water Resources Planning Organisation (WARPO) of Bangladesh and Landsat satellite images were used (Ahmed et al., 2018). The collected data from WARPO provided the areas of eroded and accreted lands for the past thirty years from 1985 to 2015. Moreover, the study used multi-temporal Landsat satellite images for the years 1985 (TM), 1995 (TM), 2005 (ETM+) and 2015 (ETM+) for the same time period (i.e. 1985 to 2015) to check the consistency of the data collected from WARPO. The satellite images were collected for the months of December and January considering the cloud cover, visibility and availability of images. The study followed raw quantized calibrated pixel values (DN) (Dewan et al., 2017) to identify the eroded and accreted land areas by separating land area from water body. The inventory map identified a total of 2693.80 km² of coastal lands that experienced erosion and/or accretion (or both erosion and accretion) over the past thirty years from 1985 to 2015. This time period corresponds to the datasets used for hydro-climatic parameters (except river discharge for which data for the past twenty years were used) of the LSCE model. The areas of change identified by the inventory map cover 5.96 % of the entire coastal area. The outputs of the LSCE model were then overlaid on the inventory map and the overlapped areas under five susceptibility classes of the model were then used for generating 'Degree of Fit' (DF) curves. The study considered 5 % degrees of freedom and assumed that the higher the percentages of high and very high susceptibility areas of the model results that overlap on the dynamic area identified by the inventory map, the greater the validity of the model and vice-versa. This method has been applied for different studies (Fernandez et al., 2003; Irigaray et al., 2007; Jimenez-Peralvarez et al., 2009) where the following equation (Equation 2) was used to generate the degree of fit curves for this study:

$$DF_i = \frac{m_i / t_i}{\sum m_i / t_i} \qquad (2)$$

where,

m_i= area occupied by the source areas (inventory map) at each susceptibility level

t_i = total area covered by that susceptibility level

3. Results

3.1. Overall susceptibility to erosion

The raster-based LSCE model generated comprehensive maps in which the levels of overall (annual average) land susceptibility of the coastal area to erosion are presented under five susceptibility classes (Fig. 4). The model identified 0.59 % (266.32 km²) and 0.02 % (10.01 km²) of the coastal lands as high and very high susceptibility to erosion, respectively, that makes 276.33 km² in total which is significant for the densely populated coastal area of the country. Remaining 5.49 %, 20.56 % and 73.34 % of lands were identified as moderate, low and very low susceptibility to erosion, respectively, by the model.

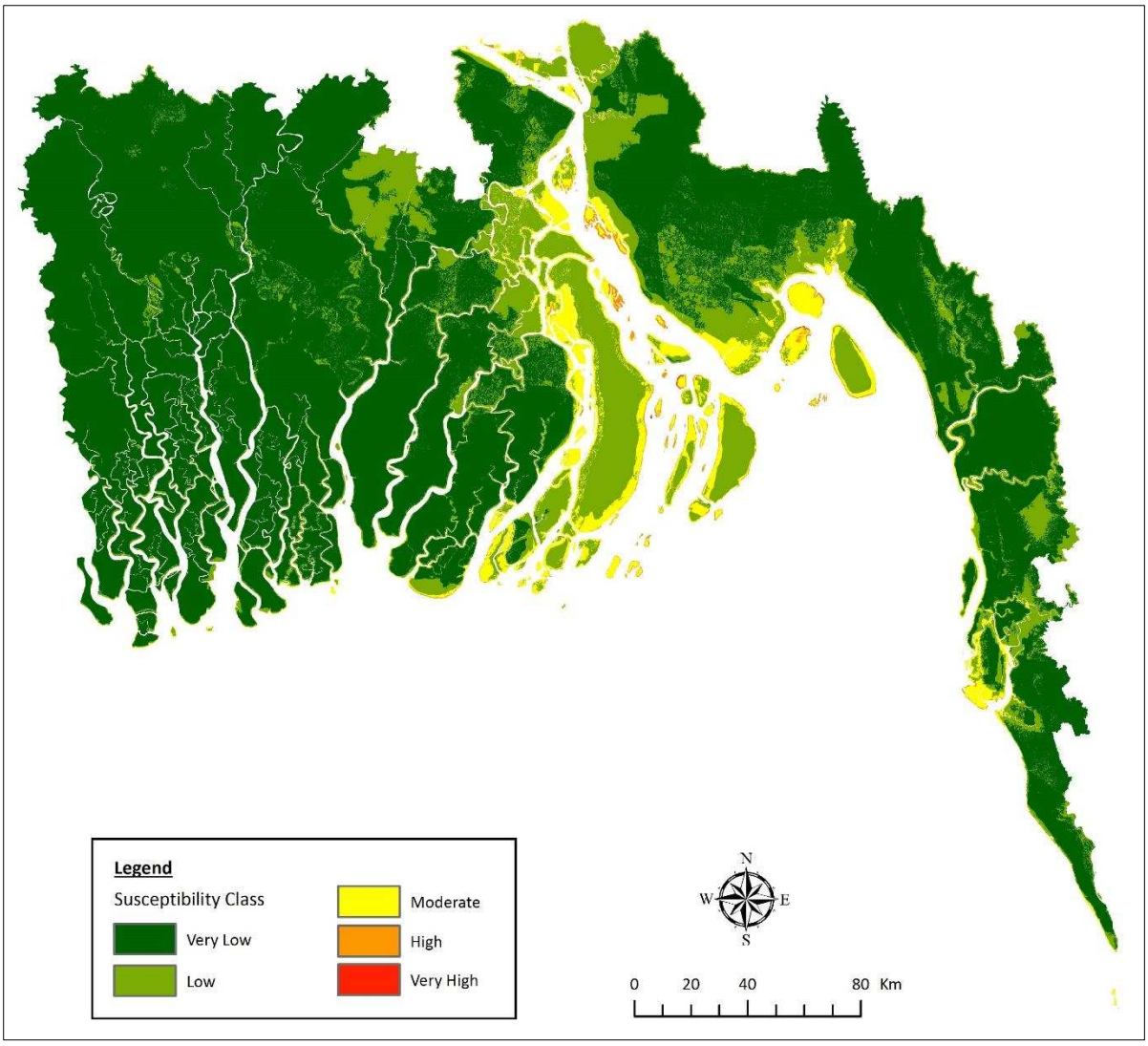

Fig. 4. Overall land susceptibility to erosion in the coastal area of Bangladesh. The outputs of the model indicate significant spatial variations in susceptibility to erosion. Most of the interior coastal lands were modelled as very low susceptibility class whereas the exterior areas showed a mix of low, moderate, high and very high susceptibility to erosion.

Spatially, the model identified most of the lands in the western coastal zone as very low and low susceptibility to erosion. Exceptions were found for the Kuakata coastal area under the Patuakhali district where a significant portion of lands were marked as moderate to high and very high susceptibility to erosion. The model outcomes for the eastern coastal zone are slightly different than the western zone for overall susceptibility to erosion. Although most of

the areas in the eastern zone were identified as very low and low susceptibility classes, some areas such as Kumira and Bhatiari of the Chittagong district, Kutubdia Island, the southern part of Moheshkhali sub-district and St. Martin Island showed moderate to high and very high susceptibility to erosion. In contrast, the most diverse erosion susceptibility was found for the central estuarine coastal area of the country that comprised all of the susceptibility classes. Low erosion susceptibility was identified for the interior parts of this central zone whereas most of the small islands were identified as moderate to high and very high susceptibility to erosion.

3.2. Seasonal variations

3.2.1. Winter

The percentages of land area under very high, high, moderate and very low susceptibility classes for winter season were identified as lower than the percentages obtained for annual average (overall) erosion susceptibility of the area (Fig. 5). For instance, the high and very high susceptibility classes were identified as 0.34 % (155.16 km^2) and 0.01 % (3.02 km^2) of the total land area, respectively, for this season. Moreover, the total land area identified as moderate susceptibility during this season was 1.48 % less than the overall annual susceptibility (Fig. 6). The results showed a total of 70.65 % of land area as very low susceptibility to erosion which was 2.69 % less than the overall susceptibility. However, the area for low susceptibility showed 24.99 % land which is 4.43 % higher than the overall susceptibility assessment. Spatially, the northern and central parts of the coastal lands were modelled as low erosion susceptibility for this season. During this season, most of the lands in the central estuarine area exhibited low susceptibility to erosion. Some small islands in the central coastal zone are classified as very high susceptibility to erosion during this season. Except for some moderate erosion susceptibility areas in Moheshkhali and the St. Martin Islands, most of the areas in the eastern coastal zone were modelled as very low erosion susceptibility. However, almost the entire western zone was identified as very low to moderate erosion susceptibility for this season.

3.2.2. Pre-monsoon

The model identified 0.33 % (150.71 km²) and 0.01 % (3.88 km²) of land areas as high and very high susceptibility to erosion, respectively, for the pre-monsoon season. These amounts are lower than the overall annual susceptibility values but are almost similar to those for the winter season. On the other hand, about 83.8 % of land was modelled as very low erosion susceptibility for this season, which is 10.46 % and 13.15 % higher than overall and winter susceptibility to erosion, respectively. Differences were also found for low and moderate susceptibility classes that are much lower (6.57 % and 3.63 % subsequently) than the average susceptibility to erosion. The western coastal zone showed a very low susceptibility to erosion during this season except for some areas in Kuakata and some small islands located in the south-western coastal zone. In contrast, the central coastal zone was mostly identified as low erosion susceptibility during this season, having significant portions of moderate, high and very high susceptibility areas (Fig. 5). The southern portions of the islands in this zone were modelled as very low susceptibility compared to other areas. However, the newly developed small islands and the shorelines of comparatively bigger islands in the central zone were identified as moderate to high and very high susceptibility to erosion during this season. A highly exceptional case was found for Urir Char and Char Piya islands in the central zone. Major parts of these newly developed lands were modelled as moderately susceptible but some areas were classified as high and very high susceptibility to erosion. Almost all of the areas in the eastern coastal zone exhibited very low to low erosion susceptibility during this season. Some areas in Moheshkhali Island were identified as moderate susceptibility to erosion as an exception in this zone.

3.2.3. Monsoon

The LSCE model identified the monsoon period as the most susceptible season to land erosion when significant amounts of high (441.8 km²) and very high (21.14 km²) susceptibility areas were noticed. A total amount of 1680.98 km² land area was identified as moderate susceptibility for this season, which is lower than winter and pre-monsoon seasons.

Considerable portions of land in the central coastal area were found as high and very high susceptibility to erosion. The lands attached to the northern, eastern and southern shorelines of most of the comparatively larger islands, namely Bhola, Hatiya, Urir Char, Jahajir Char, Char Piya, Sandwip and Monpura, were modelled as high and very high susceptibility to erosion. The southern coastline of the mentioned islands showed comparatively less susceptibility to erosion in this zone. All other small islands in the central coastal zone largely exhibited high and very high susceptibility to erosion during this season. The eastern coastal zone shows comparatively lower susceptibility than the central zone, bu indicates higher susceptibility than the western zone during this season (Fig. 5). However, the Moheshkhali and St. Martin islands in the eastern zone showed greater susceptibility to erosion than other areas during this season.

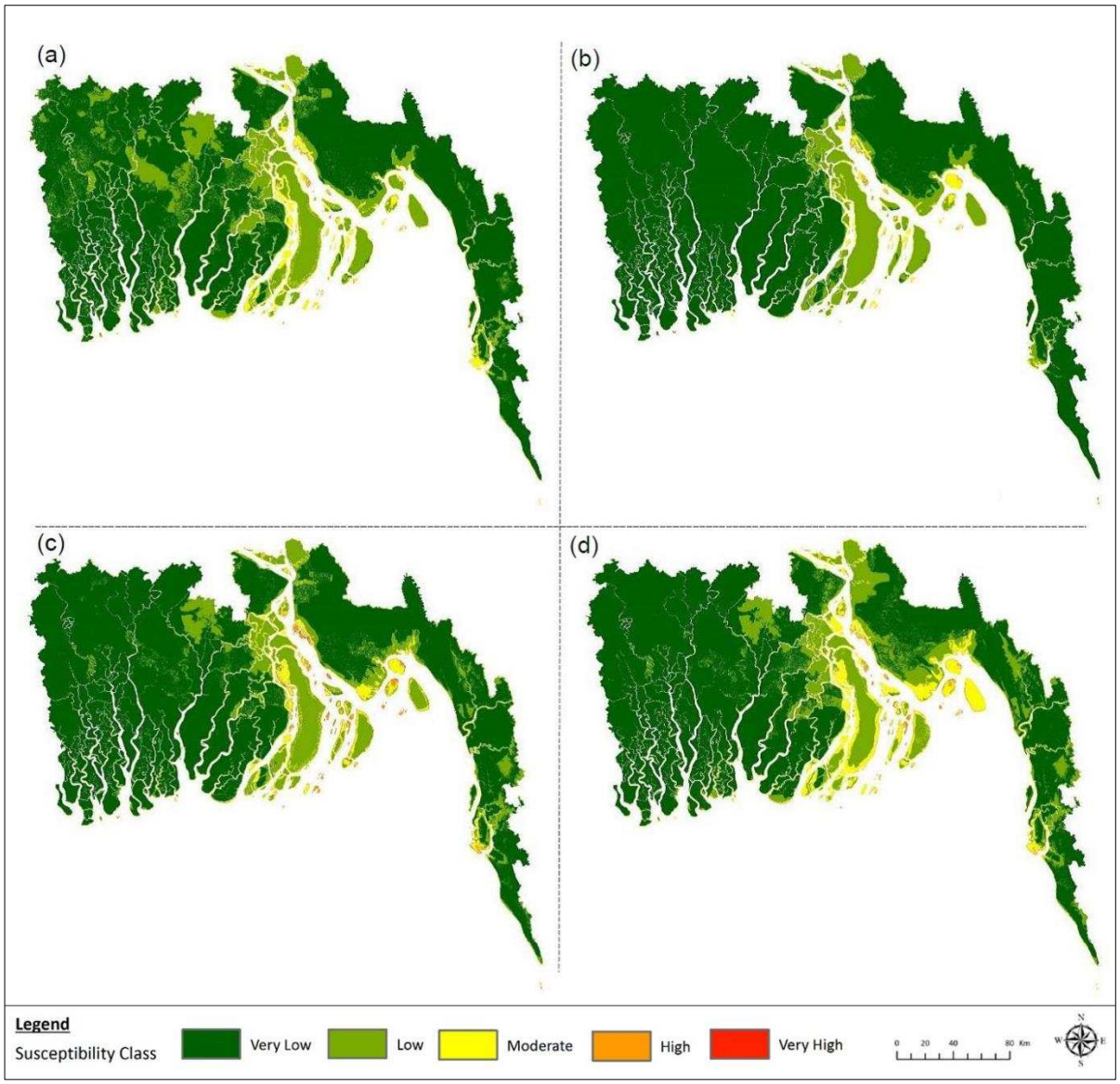

Fig. 5. Susceptibility to erosion during (a) winter, (b) pre-monsoon, (c) monsoon and (d) post-monsoon seasons in the coastal area of Bangladesh. The figure indicates spatial variations of erosion susceptibility for the seasons that are mostly governed by the varied nature of influences of the hydro-climatic forces in the area.

3.2.4. Post-monsoon

Susceptibility to erosion during the post-monsoon season showed a very similar results to those for average susceptibility. During this period, very high, high and moderate susceptibility classes showed slightly higher amounts of land compared to average susceptibility to erosion. However, very low susceptibility land area was only 3 % less than the overall susceptibility

whereas low susceptibility land area was 1.29 % more than the average erosion susceptibility. Most of the areas in the western coastal zone were identified as very low and low erosion susceptibility for the post-monsoon season. A similarity with overall susceptibility was found for the Kuakata coastal area that shows moderate to high susceptibility to erosion. Most of the islands and newly developed lands such as Sandwip, Urir Char, Jahajir Char, Monpura, Char Piya, Char Shahbaz, Char Gazaria, Char Zahiruddin, Dhal Char, Char Joman, Latar Char, Char Tazul, Sona Char and some other unnamed small islands in the central coastal zone show moderate, high and very high susceptibility to erosion during this season. Like the monsoon season, the coastal area of Moheshkhali and St. Martin islands located in the eastern zone were modelled as moderate to high and very high susceptibilityy to erosion during the post-monsoon season (Fig. 5).

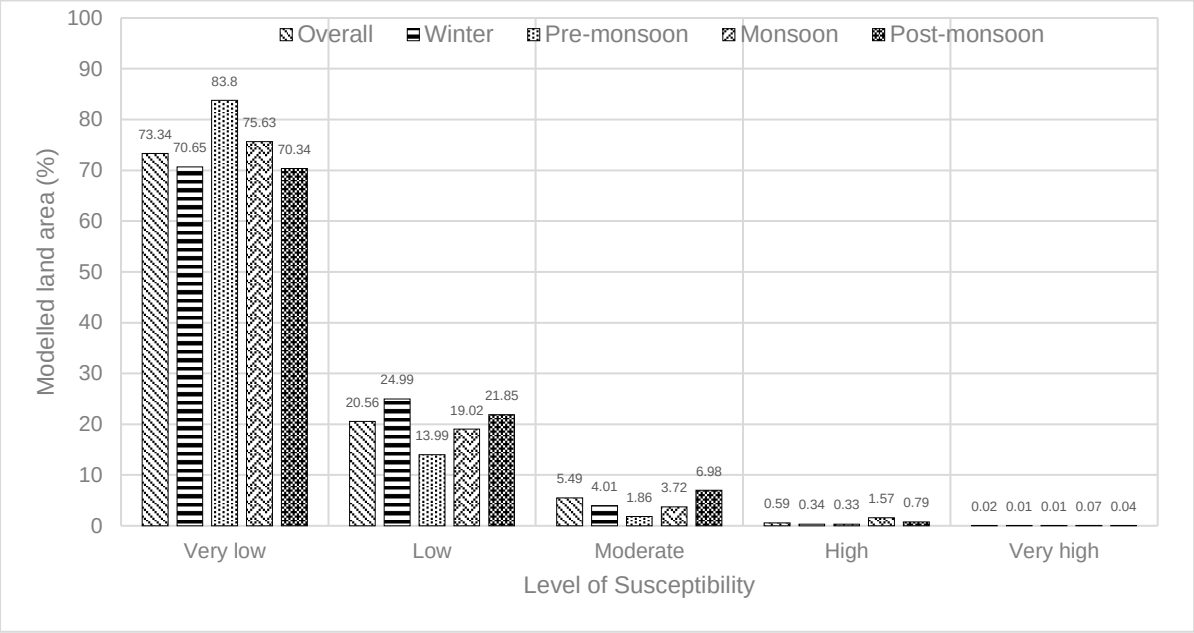

Fig. 6. Comparison of the percentages of land areas under different susceptibility classes identified for the overall year and for different seasons. The figure demonstrates higher percentages of land for high (1.57%) and very high (0.07%) susceptibility classes during the monsoon season. However, this situation is different for winter, pre-monsoon and post-monsoon seasons. These variations in seasonal susceptibility compared to the overall

conditions indicate the influence and interactions of hydro-climatic factors on erosion susceptibility in the area.

Table 2: Estimated population exposed to high risk for overall and seasonal periods. The estimation was calculated by multiplying the total amount of high and very high susceptibility lands by the average density of population (940/km²) in the area.

Time/ season	Total amount of high and very high susceptible land (km²)	Total number population at risk (estimated)
Overall	276.33	2,62,237
Winter	158.18	1,50,112
Pre-monsoon	154.59	1,46,705
Monsoon	739.27	7,01,567
Post-monsoon	375.72	3,56,558

4. Discussion

4.1. Validation of the results

The LSCE model outputs demonstrate a strong match with the areas of coastal change identified on the inventory map. The degree of fit curves (Fig. 7) and map (Fig. 8) show that 95.7 %, 96.36%, 95.05%, 95.79% and 95.06% of very high susceptibility class of the modelled areas for annual average, winter, pre-monsoon, monsoon and post-monsoon periods, respectively, overlapped with the dynamic area identified on the inventory map. Although the very high erosion susceptibility class covers 0.02 %, 0.01 %, 0.01 %, 0.07 % and 0.04 % of the total modelled area for average, winter, pre-monsoon, monsoon and post-monsoon periods, respectively (Fig. 6), most of the areas in that class (above 95%) overlapped within the area identified similarly on the inventory map (Fig. 8). On the other hand, only 0.48 %, 0.47 %, 0.92 %, 0.51 % and 0.46 % of very low erosion susceptibility class of the modelled areas for overall, winter, pre-monsoon, monsoon and post-monsoon periods, respectively, overlapped with the areas identified on the inventory map. These two opposite overlapping conditions of modelled areas with the inventory map meet the assumptions previously set for

the validation of the model. The validation also fulfils the assumptions set for low and high erosion susceptibility areas of the model for the annual average and for all the four seasons. However, the overlapped areas for moderate susceptibility class ranging from 52.89% to 66.36% for overall and all other seasons except pre-monsoon (86.93%).

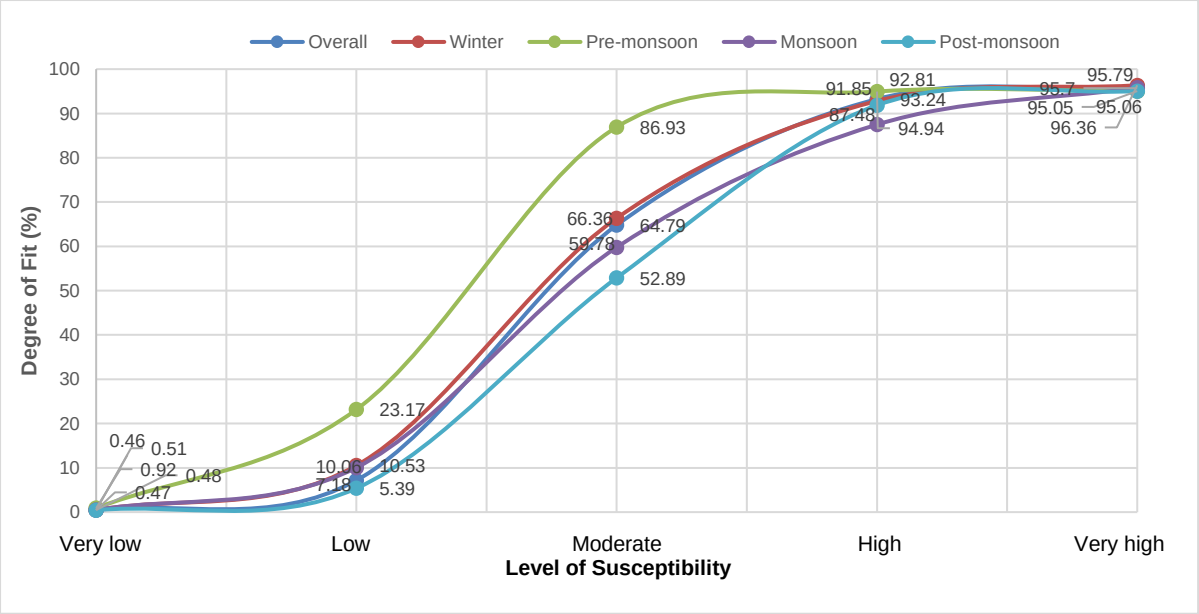

Fig. 7. Degree of fit curves for the validation of LSCE model results. The vertical axis shows the relative frequency of the degree of fit (%) to independent observations of coastal change whereas the horizontal axis indicates the levels of susceptibility identified by the LSCE model. The lines show the percentages of modelled lands that overlapped with the dynamic lands identified on the inventory map.

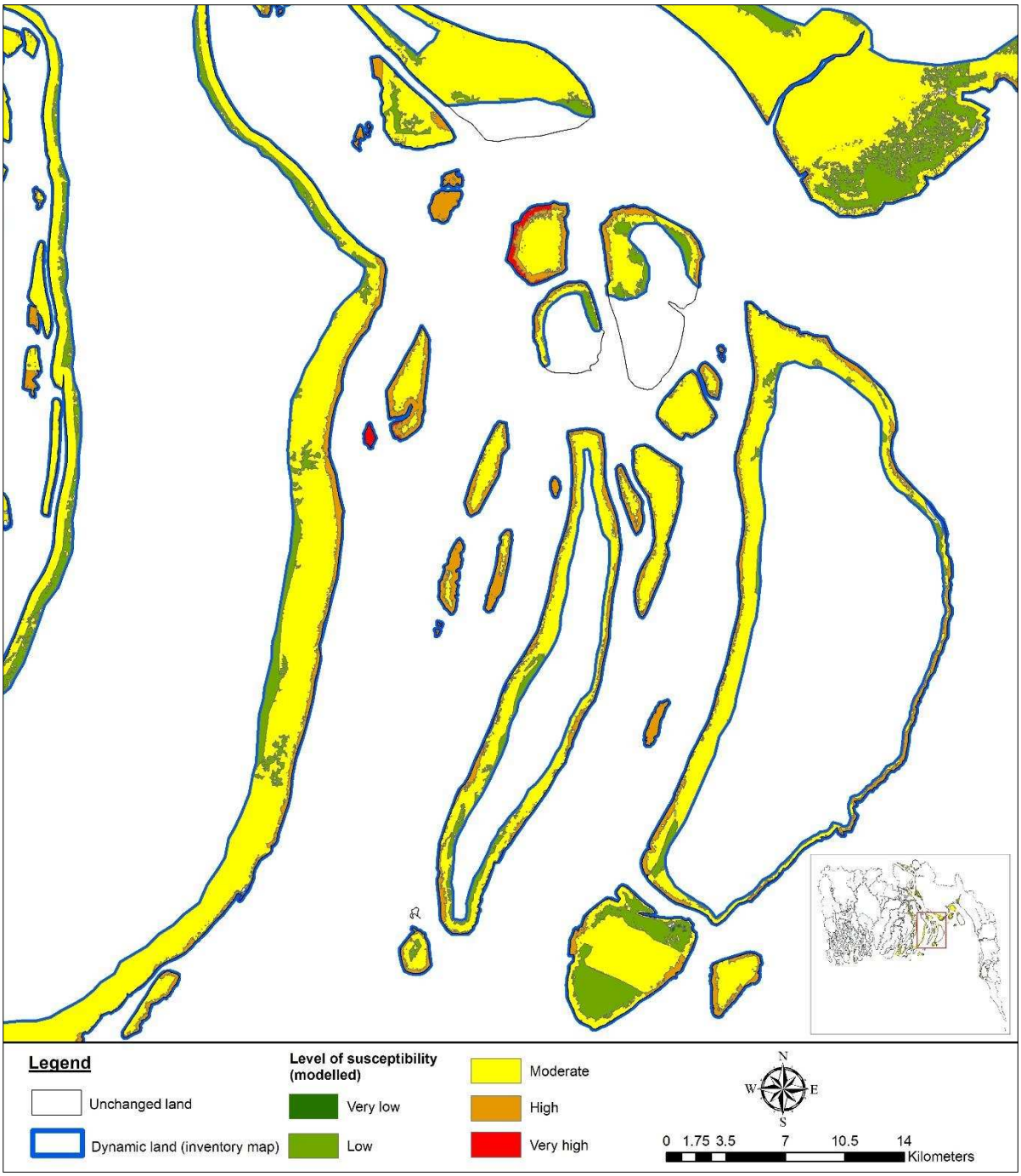

Fig. 8. Example of a zoomed-in area of the full inventory map (inset) used for validating the outputs of the LSCE model for erosion susceptibility. The figure shows the dynamic lands identified on the inventory map that experienced changes (erosion and/or accretion or the both) for different times from 1985 to 2015. The different levels of susceptibility to erosion show only the portions of land that overlapped with the dynamic land identified on the inventory map.

4.2. Impacts of hydro-climatic factors

The model results indicate significant influences of the selected hydro-climatic factors (i.e. discharge of coastal river water, mean sea level, rainfall and wind speed) on erosion susceptibility of the coastal area. More specifically, variations in erosion susceptibility for the three coastal zones were the result of the spatial and seasonal variations of hydro-climatic parameters in the area. For instance, whilst having almost similar physical conditions (i.e. surface elevation, surface geology, soil permeability) to the central zone, most of the areas in the western coastal zone were identified as having lower susceptibility to erosion. The average discharge of river water in this western zone vary from a low 13 m^3/s to a highest 6,152 m^3/s only. This low river discharge substantially reduced the level of susceptibility to erosion in this zone. Similarly, the mean sea-level data for the past thirty years from 1985 to 2015 show comparatively less variation in the western zone than other zones. However, the variation ranges from a low of 1.61 m during winter to a high of 2.77 m during the monsoon season. These situations of water discharge and mean sea level have significant impacts on the seasonal variations of erosion susceptibility in the western zone. Likewise, the pattern of rainfall that ranges from a low of 90 mm to a high of 421 mm during pre-monsoon and monsoon seasons in the western zone has potential impact on seasonal variations of erosion susceptibility. The effects of wind speeds in generating waves in this coastal zone are minimal for most of the times in a year. However, this zone experienced 3.26 m/s winds during monsoon season when, the winds blow from southwestern direction. This southwestern direction of winds along with shallo water depths consequently increase the wave actions, the ultimate result of which initiate erosion in the southern part of this zone.

The impacts of hydro-climatic drivers were noteworthy for higher erosion susceptibility in the central coastal zone compared to the western and the eastern zone. The high river discharges, high rate of sediment supply, varied bathymetric depths, varied mean sea level and continuous wave action greatly influenced the model results for higher erosion susceptibility of this zone.

The data for the past twenty years show that the Meghna estuary areas of the central zone experience discharge values as low as 3529 m^3/s during winter to as high as of 65,396 m^3/s during the monsoon season through the combined flow of the Padma (part of Ganges), the Meghna and the Jamuna (lower part of the Brahmaputra) river. Further, the varied mean sea level (vary from a low of 1.61 m during winter to a high of 3.44 m during monsoon) in the estuarine areas inundates significant portions of the land area. This higher variation of mean sea level combined with huge volume of river discharge contributes to the high rate of erosion. This situation is evident for the Sandwip channel, Urir Char and Jahajir Char areas of the zone.

Heavy rainfall during monsoon season along with high river discharge and south-westerly winds increase water level in the Meghna estuary and south-eastern parts of the central coastal zone, which accelerated the rate of erosion for most of the islands of this central zone. Although the interior parts of the coastal area experienced moderate to high range of rainfall (i.e. from a low of 122 mm to a high of 186 mm) during pre-monsoon and post-monsoon seasons, the south-eastern parts experienced a range of 540 to 659 mm of rainfall on average for the past thirty years from 1985 to 2015. The model identified a higher level of erosion susceptibility for Patharghata and the Meghna estuary areas and moderate susceptibility for the Barguna and Patuakhali coastal districts that correspond with previous research (Hossain, 2012; Sarwar and Woodroffe, 2013).

The analysis based on the data for the past thirty years infers that the influence of wind speed vary for the three coastal zones in accordance with the seasons and directions. The central zone exhibits moderate wind speed that ranges from 0.36 m/s during the post-monsoon season to 2.69 m/s during the monsoon season. Due to southern and southwesterrn directions of winds during pre-monsoon and monsoon seasons respectively, the islands and shoreline areas of the central coastal zone experiences significant wave actions. The southern part of the western zone exhibits wave actions mostly due to the southern wind during pre-monsoon

season. In contrast, the the strong southern winds blow over the land areas of the eastern coastal zone of the country and hence, have less significant impacts on erosion in this zone. Moreover, the generated waves from southwestern winds also have less significant influences in the eastern coastal zone due to favourable geomorphic features. The northern and northwestern winds have less potentials to generate waves in the three coastal zones due to their direction from land to the Bay. However, the combined effects of prevailing south and southwestern winds, river discharge and high tidal level are mostly responsible for higher erosion susceptibility in this central coastal zone than the western and eastern zones. The case of Urir Char is a perfect example, which is an offshore island in the Meghna estuary (Hussain et al., 2014). Sediments from river discharges that enter into Hatiya channel are trapped by that counter-clockwise circulation before settling in or being transported out of the Meghna estuary (Ali et al., 2007). However, the effects of hydro-climatic drivers on erosion susceptibility are less in the eastern coastal zone than the western and central zones. This is because of the presence of higher surface elevations, solid geological formations and very slow permeability of soils in the eastern zone. The shallow bathymetric depths generate waves in this zone but, due to the aforementioned reasons, the actions of waves are less effective for erosion.

4.3. Controls of underlying physical elements

The spatial and seasonal variability of the model outputs discussed relies highly on how the hydro-climatic factors interact with the underlying physical characteristics of the area. For instance, the study identified the eastern coastal zone as having lower susceptibility to erosion than the central coastal zone. Except winds and associated wave actions, the influences of all other hydro-climatic factors are less significant in the eastern zone than the central and western coastal zone. The higher surface elevations along with hard and consolidated rock, flat and unbroken coast and the longest natural beach make the zone the most stable part of the coast (Brammer, 2014). However, some parts of the zone, such as Kutubdia and

Moheshkhali islands and the upper part of Cox's Bazar district showed moderate to high and very high susceptibility to erosion due to the presence of alluvial silt and clay and the Chandina alluvium formation. Some land areas in Kutubdia and Moheshkhali islands and in the Cox's Bazar district fall below 3 m above mean sea level which makes the areas moderate to highly susceptible to erosion. The bathymetric depths of this zone vary from high to very high susceptibility class (<-5 to -10 m). Although the impacts of river discharge are very low but, wave actions have significant roles to initiate erosion due to shallow nearshore depths in this zone. Additionally, most of the areas of this zone belong to slow to moderate permeability of soils that contribute to the low erosion susceptibiltiy of the zone.

The central coastal zone is the most active and dynamic zone compared to other zones (Karim and Mimura, 2006) that correspond with the outputs of the LSCE model. Although the surface elevation of this zone ranges from 3 to 12 m for the interior and eastern parts, this value ranges from 1 to 3 m for most of the islands and newly developed lands. Together with surface elevations, the geomorphic features such as the estuarine silt and clay deposits, newly formed ocean and riverine deposits, tidal sands, deltaic sands, beach and sand dunes and alluvial sands in the exterior parts of the zone contributed to the higher level of susceptibility to erosion in that islands and newly developed lands. The islands are highly susceptible to erosion due to silt- and clay-dominated soft unconsolidated sediments. An example can be cited of Hatiya Island which is composed of Quaternary alluvial deposits of silt, sand and clay. The morphology of the island is changing rapidly due to its alluvial lithology which is very sensitive to river discharge, tides and waves (Ghosh et al., 2015). Along with geomorphic features and soil characteristics, the varied bathymetry of the zone is thought to be favourable to erosion due to the high volume of river discharge. Moreover, the bathymetric depths of the central zone vary from a higher depth in the interior coast (i.e. up to -44.84 m near the upper portion of the Sandwip island and in the Meghna river channels) to a lower depth (i.e. -10 m) in the exterior coast. This high depth in the Meghna estuarine area and northern portions of the

islands created thalwegs (MES II, 2001; BN, 2010; GMRT, 2017). However, the exterior coast of the central zone experiences higher wave actions due to lower batymetric depths, comparing to the internal coast.

The hydro-climatic parameters act differently in the western coastal zone than in the central and eastern zones. This situation is highly governed by the existence of Mangrove vegetation in the area. Although the surface elevation of this zone shows a mixed range of 0 to 6 m above mean sea level, mangrove vegetation acts as an active agent of protection for the area from erosion and plays a vital role for accretion in this zone (Aziz and Paul, 2015; Islam and Rahman, 2015). Mangrove vegetation also creates a barrier against wave action (Umitsu, 1997). The most western part (the Sundarbans Mangrove) of the zone is composed of valley alluvium and colluvium, tidal mud, marsh clay and peat and mangrove swamp deposits. Along with geomorphic features, the presence of fine sand and silt in the beds of this coastal zone (Sarker, et al., 2011) indicates a high rate of siltation (MES II, 2001) which substantially reduced the erosion susceptibility of this zone. Additionally, the soils in this zone are characterised as having very slow to moderate permeability, and are highly resistent to erosion. Consequently, the susceptibility to erosion is reduced. Due to the excessive amount of siltation near the shoreline, most of the areas belong to the very low (<-5 m) to low (-5 to -10 m) nearshore bathymetric depths. The depths of the rivers at the interior parts of this zone are higher than the exterior coast (i.e. -10 to more than -20 meters in some places). Moreover, the interior coastal lands are very far from the existing shoreline that are not highly influenced by the wave action, and hence resembles lower susceptibility to erosion. However, the lower depths near shoreline generate waves and hence, significantly contribute to erosion in Barguna, Patuakhali and Bhola areas of the coast.

4.4. Roles of preparatory factors

Although very little is evident on the specific preparatory factors responsible for the susceptibility to erosion in the coastal area, this study addressed the influence of accretion (sedimentation) and defence structures on the susceptibility to erosion. A number of moderators on accretion were used for the LSCE model that substantially reduced the scores of susceptibility in the model for different areas of the coast. For example, the accretion moderator used in the model for Ramgati and Khaser Haat in the Patuakhali district significantly reduced the level of erosion susceptibility from very high to high and moderate classes. Moreover, the accretion moderator applied for Nujhum Dwip, Char Gazaria, Char Shahbaz, Char Halim and Char Kukri Mukri located in central coastal area reduced the susceptibility scores for those areas. Similarly, the LSCE model addressed the issue of defence structures constructed by the government of Bangladesh from time to time, by generating accretion moderators especially for the Meghna estuary in the model domain. It is reported that more than one billion tons of sediment are carried by the Ganges, the Brahmaputra and the Meghna each year, of which a significant portion deposits on the tidal plain of the coast (Goodbred and Kuehl, 2000). Concentration of suspended sediment in the lower reaches of Shahbajpur channel is very high (about 2000 ppm) (MES II, 2001; Sokolewicz and Louters, 2007). Consequently, the high rate of sedimentation significantly reduced the levels of erosion susceptibility in this area of the central coastal zone.

5. Conclusion

The study modelled the interior part of the coast as very low to low susceptibility to erosion, and the exterior part of the coast as moderate to high and very high susceptibility to erosion. Based on the zones, the central estuarine zone was identified as highly susceptible to erosion whereas the eastern and the western zones of the coast were comparatively identified as very low to low erosion susceptibility. The results demonstrate that overall 276.33 km² land area is highly susceptible to erosion. The approximate population living in area at high risk of erosion (Table 2) is noteworthy for the country's socio-economic and demographic context. However,

the modelled results strongly rely on the availability of data, use of model parameters, definition of class values and the given weights for the parameters. Hence, emphasis was given in choosing model parameters, classifying the data and assigning them weights before the model was run. Moreover, the framework of the model was designed to facilitate the analysis of prevailing impacts of hydro-climatic factors on erosion susceptibility. However, the LSCE model framework provides a new insight on assessing future erosion susceptibility, which may be applied to any coastal lands around the world that are prone to likely changes in future hydro-climatic factors.

The assessment identified dominant regional as well as seasonal drivers of susceptibility to erosion. In the western coastal zone, along with a low impact of hydro-climatic drivers such as coastal river discharge, rainfall, mean sea level, wind speed and wave action, other drivers such as low permeability fine and silt deposits and varied bathymetry are identified as main drivers of susceptibility to erosion. In contrast, low surface elevations, newly formed alluvial deposits, high permeability soils, wave actions, varied bathymetry, high river discharge, variations in mean sea level, heavy rainfall, high rate of sedimentation and embankments (defence structure) are active drivers of susceptibility to erosion in the central coastal zone. In case of eastern zone, high surface elevations, hard and consolidated rocks, beach and sand dune, lower bathymetric depths, heavy rainfall and development works (e.g. marine drive) are the main drivers of susceptibility to erosion. The effects of these drivers vary for the four seasons in which winter is characterised by low flow of coastal river water, absence of cyclone and storm surges, less rainfall, low wind speeds and less wave action. The drivers are similar for the pre-monsoon and post-monsoon seasons, whereas the monsoon season is characterized by high river discharge, continuous wave action, heavy rainfall and significant variations in mean sea level.

The outputs of the LSCE model offer coastal managers and policy makers vital inputs in assessing erosion susceptibility of dynamic coastal areas, which in principle can be applied around the world. The assessment of susceptibility could offer insights into the underlying causes and the impacts of hydro-climatic factors on the susceptibility to coastal erosion. This LSCE model offers a new platform with which to assess likely impacts of future hydro-climatic changes on future erosion susceptibility of the coastal areas around the world. Additionally, this research is important for the coastal managers to take initiatives in protecting coastal lands and preventing the shoreline from potential erosion. The model results for the study area could also be vital for implementing re-settlement plans for newly developed coastal islands and landmasses attached to the mainland in the Meghna estuarine area of the coast.

Acknowledgement

The current research is a part of doctoral thesis at the University of Leeds, United Kingdom. The assessment of future susceptibility to erosion in the studied coastal area is also included in this PhD research. The authors are thankful to the University of Leeds for funding the research under Leeds International Research Scholarships (LIRS) scheme.

References

Addo, A.K., Walkden, M., Mills, J.P., 2008. Detection, measurement and prediction of shoreline recession in Accra, Ghana. ISPRS J. Photogramm. Remote Sens. 63 (5), 543–558.

Ahmed, G.U., 1999. Decision Analysis for Bangladesh Coastal Afforestation, Master thesis, University of Toronto, Ontario.

Ahmed, A., Drake, F., Nawaz, R., Woulds, C., 2018. Where is the coast? Monitoring coastal land dynamics in Bangladesh: An integrated management approach using GIS and remote sensing techniques. Ocean and Coastal Management. 151, 10–24.

Alam, M.S., Uddin, K., 2013. A Study of Morphological Changes in the Coastal Areas and Offshore Islands of Bangladesh Using Remote Sensing. American Journal of Geographic Information System. 2(1), 15-18. DOI: 10.5923/j.ajgis.20130201.03

Ali, A., 1999. Climate change impacts and adaptation assessment in Bangladesh. Clim. Res. 12, 109–116.

Ali, A., Mynett, A. E., Azam, M. H., 2007. Sediment Dynamics in the Meghna Estuary, Bangladesh: A Model Study. J. Waterway, Port, Coastal, Ocean Eng. 133(4), 255-263.

Alves, F.L., Coelho, C., Coelho, C.D., Pinto P., 2011. Modelling Coastal Vulnerabilities- Tool for Decision Support System at Inter-municipality Level. Journal of Coastal Research. 64, 966-970.

Azab, M.A., Noor, A.M., 2003. Change detection of the North Sinai coast by using remote sensing and Geographic Information System. Proc. 4th International Conference and Exhibition for Environmental Technologies, Cairo, Egypt, 30 Sep tember to 2 October, pp. 118-124.

Aziz, A., Paul, A.R., 2015. Bangladesh Sundarbans: Present Status of the Environment and Biota. Diversity. **7**, 242-269. Doi: 10.3390/d7030242

Balica, S.F., Wright, N.G., van der Meulen, F., 2012. A flood vulnerability index for coastal cities and its use in assessing climate change impacts. Natural Hazards. 52, 1-33.

BARC (Bangladesh Agricultural Research Council), 2016. Land Resources Information and Maps of Bangladesh. http://maps.barcapps.gov.bd/index.php (Accessed on: 10 April 2018).

Barua, D.K., 1997. The active delta of the ganges-Brahmaputra rivers: dynamics of its present formations. Mar. Geod. 20 (1), 1–12. http://dx.doi.org/10.1080/01490419709388091.

BBS (Bangladesh Bureau of Statistics), 2011. Population census of Bangladesh, statistical and information division, ministry of planning.

BBS (Bangladesh Bureau of Statistics), 2015. Population Monograph of Bangladesh, Population density and vulnerability: A challenge for sustainable development of Bangladesh, volume 7.

Bird, E., 2008. Coastal Geomorphology: An Introduction. John Wiley & Sons Ltd, UK.

BIWTA (Bangladesh Inland Water Transport Authority), 2017. Department of Hydrography, Bangladesh Inland Water Transport Authority, Dhaka, Bangladesh.

BMD (Bangladesh Meteorological Department), 2016. Climate Data Portal. http://bmd.wowspace.org/team/homex.php (Accessed on: 25 October 2016).

BN (Bangladesh Navy), 2010. Chart catalogue (HP 001), Bangladesh Navy Hydrographic and Oceanographic Center, Chittagong, http://bnhoc.navy.mil.bd/ (Accessed on: 10 October 2016).

Boak, E.H. and Turner, I.L., 2005. Shoreline Definition and Detection: A Review. Journal of Coastal Research, 21(4), 688–703.

Boori, M. S., 2010. Coastal vulnerability, adaptation and risk assessment due to environmental change in Apodi Mossoro estuary, Northeast Brazil, International Journal of Geomatics and Geosciences. 1(3), 620-638.

Brammer, H., 2014. Bangladesh's dynamic coastal regions and sea-level rise. Climate Risk Management. 1, 51–62.

Bryan, B., Harvey, N., Belperio, T., Bourman, B., 2001. Distributed process modeling for regional assessment of coastal vulnerability to sea level rise. Environmental Modeling and Assessment. 6, 57-65.

BWDB (Bangladesh Water Development Board), 2016. Processing and Flood Forecasting Circle, Hydrology Section, Dhaka, Bangladesh.

Cai, H., Lam, N.S.N., Zou, L., Qiang, Y., Li, K., 2016. Assessing Community Resilience to Coastal Hazards in the Lower Mississippi River Basin. Water. 8, 46.

Chowdhury, S.Q., 2013. Coastal Erosion, Banglapedia, Asiatic Society of Bangladesh.

Chowdhury, S.R., Tripathi, N.K., 2013. Coastal erosion and accretion in Pak Phanang, Thailand by GIS analysis of maps and satellite imagery. Songklanakarin journal of science and technology. 35 (6), 739-748.

Chung, C.F., Fabbri, A.G., 2003. Validation of Spatial Prediction Models for Landslide Hazard Mapping. Natural Hazards. 30, 451-472.

Dawson, R.J., Dickson, M., Nicholls, R.J., Hall, J., Walkden, M.J.A., Stansby, P.K., Mokrech, M., Richards, J., Zhou, J., Milligan, J., Jordan, A., Pearson, S., Ress, J., Bates, P.D., Koukoulas, S., Watkinson, A., 2009. Integrated analysis of risks of coastal flooding cliff erosion under scenarios of long term change. Climate Change. 95 (1-2), 249-288.

Dewan, A., Corner, R., Saleem, A., Rahman, M.M., Haider, M.R., Rahman, M.M., Sarker, M.H., 2017. Assessing channel changes of the Ganges-Padma River system in Bangladesh using Landsat and hydrological data. Geomorphology. 276, 257-279.

Dolan, R., Hayden, B.P., May, P., May, S., 1980. The reliability of shoreline change measurements from aerial photographs. Shore and Beach. 48(4), 22-29.

Fernandez, T., Irigaray, C, El-Hamdouni, R, Chacon, J., 2003. Methodology for landslide susceptibility mapping by means of a GIS. Application to the Contraviesa area (Granada, Spain). Nat Hazards. 30, 297–308.

Fernandez-Nunez, M., Diaz-Cuevas, P., Ojeda, J., Prieto, A., Sanchez-Carnero, N., 2015. Multipurpose line for mapping coastal information using a data model: the Andalusian coast (Spain). J. Coast. Conserv. 19, 461-474.

Fitton, J.M., Hansom, J.D. and Rennie, A.F., 2016. A National Coastal Erosion Susceptibility Model for Scotland. Ocean and Coastal Management, 132, 80-89.

Fitzgerald, D. M., Fenster, M. S., Argow, B. A., Buynevich, I. V., 2008. Coastal Impacts Due to Sea-Level Rise. Annual Review of Earth and Planetary Sciences. 36, 601-647.

Ghosh, M.K., Kumar, L., Roy, C., 2015. Monitoring the coastline change of Hatiya Island in Bangladesh using remote sensing techniques. ISPRS J. Photogramm. Remote Sens. 101, 137–144.

Global Wind Atlas, 2017. Wind frequency rose, https://globalwindatlas.info/area/Bangladesh (Accessed on: 16 November 2017).

GMRT (Global Multi-Resolution Topography), 2017. Bathymetry, https://www.gmrt.org/ (Accessed on: 16 January 2017).

Goodbred, J., Kuehl, S.A., 2000. Enormous Ganges-Brahmaputra sediment discharge during strengthened early Holocene monsoon. Geology, 28, 1083-1086.

Gornitz, V.M., 1990. Vulnerability of the East Coast, USA to future sea level rise. J. Coast. Res. 9, 201-237.

Harvey, N., Woodroffe, C.D., 2008. Australian approaches to coastal vulnerability assessment. Sustain. Sci. 3, 67-87.

Hegde, A.V., Reju, V.R., 2007. Development of coastal vulnerability index for Mangalore Coast, India. J. Coast. Res. 235, 1106-1111.

Hegde, A.V., 2010. Coastal erosion and mitigation methods - global state of art. Indian Journal of Geo-Marine Sciences. 39(4), 521-530.

Hofer, T., Messerli, B., 2006. Floods in Bangladesh: History, Dynamics and Rethinking the Role of the Himalayas. United Nations University Press, Tokyo, Japan.

Hossain, M.M., 2012. Storm surges and coastal erosion in Bangladesh -State of the system, climate change impacts and 'low regret' adaptation measures. Unpublished Master Thesis, Leibniz University, Germany.

Huq, S., Karim, Z., Asaduzzaman, M., Mahtab, F. (eds.), 1999. Vulnerability and Adaptation to Climate Change for Bangladesh, first ed. Springer, The Netherlands. Doi: 10.1007/978-94-015-9325-0

Hussain, M. A., Tajim, Y., Gunasekara, K., Rana, S., Hasan R., 2014. Recent coastline changes at the eastern part of the Meghna Estuary using PALSAR and Landsat images. Paper presented at 7th IGRSM International Remote Sensing & GIS Conference and Exhibition.

IPCC (Intergovernmental Panel on Climate Change), 2007a.Climate change, impacts, adaptation and vulnerability. Contribution of working group II to the fourth assessment report of the intergovernmental panel on climate change. In: Parry M.L., Canziani O.F., Palutikof J.P., van der Linden P.J., Hanson C.E. (eds.) Intergovernmental Panel on Climate Change (IPCC). Cambridge University Press, New York.

IPCC (Intergovernmental Panel on Climate Change), 2007b. Intergovernmental panel on climate change, AR4, fourth assessment report: Climate Change 2007.

Iqubal, K.F., Ali, S., 2011. Land Loss Mapping of Manpura Island: An Integrated Approach Using Remote Sensing and GIS. Journal of State University of Bangladesh. 3(1), 16-21.

Irigaray, C., Fernandez, T., El-Hamdouni, R., Chacon, J., 2007. Evaluation and validation of landslide-susceptibility maps obtained by a GIS matrix method: examples from the Betic Cordillera (southern Spain). Nat Hazards. 41, 61–79.

Islam, M.R., 2004. Where land meets the sea: a profile of the coastal zone of Bangladesh (Ed). The University Press Limited, Dhaka. P. 317.

Islam, M.R., Ahmad, M., Huq, H., Osman, M.S., 2006. State of the coast 2006, Program Development Office for Integrated Coastal Zone Management Plan Project, Water Resources Planning Organization, Dhaka.

Islam, M.S.N., 2008. Cultural Landscape Changing due to Anthropogenic Influences on Surface Water and Threats to Mangrove Wetland Ecosystems: A Case Study on the Sundarbans, Bangladesh. PhD thesis. Brandenburg University of Technology, Cottbus.

Islam, A.Z.M. Z., Kabir, S. M. H., Sharifee, M.N.H., 2013. High-tide Coastline Method to Study the Stability of Kuakata Coast of Bangladesh Using Remote Sensing Techniques. Asian Journal of Geoinformatics. 13 (1), 23-29.

Islam, S.A., Rahman, M.M., 2015. Coastal afforestation in Bangladesh to combat climate change induced hazards. J. Sci. Technol. Environ. Inform. 02(01), 13-25.

Islam, M.A., Mitra, D., Dewan, A., Akhter, S.H., 2016. Coastal multi-hazard vulnerability assessment along the Ganges deltaic coast of Bangladesh: A geospatial approach. Ocean and Coastal Management. 127, 1-15.

IWFM (Institute of Water and Flood Management), 2012. Component 3: Study on residual flow in the Bay of Bengal considering future climate change induced hydro-meteorological scenarios. Project report, Climate Change Study Cell, 1-36.

Jimenez-Peralvarez, J.D., Irigaray, C., Hamdouni R. E., Chacon, J., 2009. Building models for automatic landslide-susceptibility analysis, mapping and validation in ArcGIS. Nat Hazards. 50, 571-590. DOI 10.1007/s11069-008-9305-8

Jimmy, O.A., 2010. An Assessment of Recent Changes in the Niger Delta Coastline Using Satellite Imagery. Journal of Sustainable Development, 3(4), 277-296.

Karim, M.F., Mimura, N., 2006. Sea Level Rise in the Bay of Bengal: Its Impacts and Adaptations in Bangladesh. Center for Water Environment Studies, Ibaraki University, Hitachi, Ibaraki 316-8511, Japan. Microsoft PowerPoint –Poster for IOC.

Krantz M., 1999. Coastal erosion on the island of Bhola, Bangladesh, Earth Science Center, Goteborg University, Sweden.

Khan, S.R., 2008. Sandwip-Urir Char-Noakhali cross dam for long-term food security, The Daily Star,<http://www.thedailystar.net/news-detail-33780> (Accessed on: 04 June 2017).

Khan, S.R., 2012. Cyclone Hazard in Bangladesh, Background Information on the Storm Surge Modelling. <http://websitetools.net/googlekeyword/word/cyclone+vs+tsunami>. (Accessed on: 18 May 2017).

Klein, R.J.T., Nicholls, R.J., 1999. Assessment of coastal vulnerability to climate change. Ambio. 28, 2182-2187.

Lins-de-Barros, F.M., Muehe, D., 2011. The smartline approach to coastal vulnerability and social risk assessment applied to a segment of the east coast of Rio de Janeiro State, Brazil. J. Coast. Conserv. 17, 211-223.

Masatomo, U., 2009. Landforms and floods in the Ganges delta and coastal lowland of Bangladesh. Marine Geodesy. 20 (1), 77-87.

Mazaheri, S., Ghaderi, Z., 2011. Shallow water wave characteristics in Persian Gulf. Journal of Coastal Research, Special Issue 64, 572 – 575.

Mcfeeters, S. K., 1996. The use of the Normalized Difference Water Index (NDWI) in the delineation of open water features. International Journal of Remote Sensing, 17(7), 1425–1432. Doi:10.1080/01431169608948714

McLaughlin, S., Cooper, J.A.G., 2010. A multi-scale coastal vulnerability index: a tool for coastal managers? Environmental Hazards. 9, 233–248.

MES II (Meghna Estuary Study II), 2001. Hydro-morphological dynamics of the Meghna Estuary, Meghan Estuary Study (MES II). Prepared for BWDB, Dhaka, Bangladesh.

MGDS (Marine Geoscience Data System), 2017. Global Multi-Resolution Topography Data Synthesis. http://www.marine-geo.org/portals/gmrt/ (Accessed on: 16 February 2017).

Mikhailov, V.N., Dotsenko, M.A., 2007. Processes of delta formation in the mouth area of the Ganges and Brahmaputra rivers. Water Resources. 34(4), 385–400.

Minar, M.H., Hossain, M. B., Shamsuddin, M.D., 2013. Climate Change and Coastal Zone of Bangladesh: Vulnerability, Resilience and Adaptability. Middle-East Journal of Scientific Research 13 (1): 114-120. DOI: 10.5829/idosi.mejsr.2013.13.1.64121

MoEF (Ministry of Environment and Forests, Bangladesh), 2007. Bangladesh: National Programme of Action for Protection of the Coastal and Marine Environment from Land-Based Activities. http://www.doebd.org/npa draft.pdf. (Accessed on: 15 July 2016).

MoWR (Ministry of Water Resources), 2005. Coastal Zone Policy. Ministry of Water Resources, Government of the People's Republic of Bangladesh.

MPI (Ministry for Primary Industries), 2017. Plantation Forestry Erosion Susceptibility Classification: Risk assessment for the National Environmental Standards for Plantation Forestry, MPI Technical – Paper No: 2017/47, New Zealand.

Naylor, L.A., Spencer, T., Lane, S.N., Darby, S.E., Magilligan, F.J., Macklin, M.G., Möller, I., 2017. Stormy geomorphology: geomorphic contributions in an age of climate extremes. Earth Surf. Process. Landforms. 42,166–190.

Palinkas, C. M., Nittrouer, C. A., Walsh, J. P., 2006. Inner-shelf sedimentation in the Gulf of Papua, New Guinea: a mud-rich shallow shelf setting. Journal of Coastal Research, 22(4), 760–772.

Parvin, G.A., Takahashi, F., Shaw, R., 2008. Coastal Hazards and Community-Coping Methods in Bangladesh. Journal of Coastal Conservation. 12(4), 181-193.

PDO-ICZMP (Program Development Office for Integrated Coastal Zone Management Plan), 2006. Draft Coastal Development Strategy, Water Resources Planning Organization, Ministry of Water Resources, Bangladesh.

Potdar, S.S., Srivastava, R., Nagaraju, M.S.S., Prasad, J., Saxena, R. K., 2003. Mapping of erosional soil loss in Nanda-Khairi watershed of Nagpur district of Maharashtra using remotely sensed data and GIS techniques. Agropedology. 13, 10–18.

Prabaharan, S., Raju, K. S., Lakshumanan, C., Ramalingam, M., 2010. Remote Sensing and GIS Applications on Change Detection Study in Coastal Zone Using Multi Temporal Satellite Data. Int. J. of Geomatics and Geosciences. 1(2), 159-166.

PSMSL (Permanent Service for Mean Sea Level), 2017. Obtaining Tide Gauge Data. http://www.psmsl.org/data/obtaining/ (Accessed on: 11 January 2017).

Rabbani, G., Rahman A. A., Nazria I., 2010. Climate Change and Sea Level Rise: Issues and Challenges for Coastal Communities in the Indian Ocean Region, Technical paper, The Henry L. Stimson Center, USA.

Ramieri, E., Hartley, A. B., Filipe, D. S., Ana, G., Mikael, H., Pasi, L., Natasha, M., Monia, S., 2011. Methods for assessing coastal vulnerability to climate change. ETC CCA Technical Paper, European Environment Agency.

Reeder-Myers, L.A., 2015. Cultural Heritage at Risk in the twenty-first century: a vulnerability assessment of coastal archaeological sites in the United States. J. Isl. Coast. Archaeol. 0, 1-10.

RRCAP (Regional Resources Centre for Asian and the Pacific), 2001. Bangladesh: State of the Environment 2001, Natural Disasters, 93-117.

Saha, S.K., Singh, B.M., 1991. Soil erosion assessment and mapping of Aglar River watershed (U.P.) using remote sensing technique. Journal of the Indian Society of Remote Sensing. 19, 67–76.

Saunders, W., Glassey, P., 2007. Guidelines for assessing planning policy and consent requirements for landslide prone land. GNS Science Miscellaneous Series 7.

Sarker, M. H., Akter, J., Ferdous, M. R., Noor, F., 2011. Sediment dispersal processes and management in coping with climate change in the Meghna Estuary, Bangladesh. Proceedings of the ICCE Workshop held at Hyderabad, India, September 2009). IAHS Publ. 349.

Sarker, M.H., Akter, J., Rahman, M.M., 2015. Century-Scale Dynamics of the Bengal Delta and Future Development. Proc. 4th International Conference on Water & Flood Management (ICWFM-2013), Dhaka, Bangladesh, 9-11 March, p. (on CDROM).

Sarwar, M., Woodroffe, C.D., 2013. Rates of shoreline change along the coast of Bangladesh. Journal of Coastal Conservation, 17 (3), 515-526.

SDC (Swiss Agency for Development and Cooperation), 2010. Disaster Risk Reduction Programme for Bangladesh 2010–2012.

Shamsuddoha, M., Chowdhury, R.K., 2007. Climate Change Impact and Disaster Vulnerabilities in the Coastal areas of Bangladesh, first ed. COAST Trust, Dhaka, Bangladesh.

Shibly, M.A., Takewaka, S., 2012. Morphological changes along Bangladesh coast derived from satellite images. Proc. of Coastal Engineering, JSCE, 3, pp. 41-45.

Shifeng, H., Jiren, L. and Mei, X., 2002. The dynamic remote sensing monitoring of eight outlets in Pearl River estuary. In Asian Conference on Remote Sensing. Available online at: http://www.gisdevelopment.net/aars/acrs/2002/pos3/286.pdf

Smith, J., 2012. A drop in the ocean. Geophy. Res. Lett.http://dx.doi.org/10.1029/2012GL053055.

Sokolewicz, M., Louters, T., 2007. Hydro-morphological processes in the Meghna Estuary, Bangladesh. In: Proceeding of International Conference on Water and Flood and Management (Dhaka, Bangladesh), pp. 327–334.

SoB (Survey of Bangladesh), 2016. Geodetic control points, Geodetic survey. http://www.sob.gov.bd/ (Accessed on: 14 March 2016).

Taguchi, Y., Hussain, M.A., Tajima, Y., Hossain, M. A., Rana, S., Islam, A.K.M.S., Habib, M.A., 2013. Detecting Recent Coastline Changes around the Urir Char Island at the Eastern Part of Meghna Estuary Using PALSAR Images. Proc. of the 4th International Conference on Water and Flood Management Dhaka, Bangladesh, 9-11 March, p. (on CDROM).

UHSCL (University of Hawaii Sea Level Center), 2017. University of Hawaii Legacy Data Portal. https://uhslc.soest.hawaii.edu/datainfo/ (Accessed on 22 June 2017).

Umitsu, M., 1997. Landforms and floods in the Ganges delta and coastal lowland of Bangladesh. Marine Geodesy. 20 (1), 77-87.

Unnikrishnan, A.S., Shankar, D., 2007. Are sea-level-rise trends along the coasts of the north Indian Ocean consistent with global estimates? Global Planet. Change 57 (3–4), 301–307.

USGS (United States Geological Survey), 2001. Digital geologic and geophysical data of Bangladesh. http://pubs.usgs.gov/ (Accessed on: 17 August 2016).

USGS (United States Geological Survey), 2017. Digital Elevation Model. https://earthexplorer.usgs.gov/ (Accessed on: 20 January 2017).

Van-Westen, C.J., 2000. The modelling of landslide hazards using GIS. SurvGeophys. 21, 241–255.

Verghese, B. G., 1999. Waters of Hope: From Vision to Reality in Himalaya-Ganga Development Cooperation. The University Press Limited, Dhaka, Bangladesh.

Viles, H., Spencer, T., 1995. Coastal problems. London, p. 350.

Wang, L.T., 2003. Delaware inland bays shoreline extraction using Landsat 7 satellite imagery. Proc. of Workshop on Digital Mapping Techniques, USGS Open File Report 03-471. p.4.

Warrick, R.A., Ahmad O.K. (ed.), 1996. ‘’The implications of climate and sea-level change for Bangladesh’’, The Netherlands: Kluwer Academic Publishers, p. 416.

WARPO (Water Resources Planning Organization), 2004. Where land meets the sea- a profile of the coastal zone of Bangladesh. Dhaka University Press Limited, Dhaka, Bangladesh.

White, K., El-Asmar, H.M., 1999. Monitoring changing position of coastline using Thematic Mapper imagery, an example from the Nile Delta. Geomorphology. 29 (1-2), 93-105.

Zoran, M., Anderson, E., 2006. The use of Multi-Temporal and Multi-spectral Satellite data for Change Detection Analysis of the Romanian Black Sea coastal Zone, J. of Optoelectronics and Advanced Materials, 8(1), 252-256.